

AFOSR-TR- 84-1228

(12)

**ARVIN/CALSPAN**

AD-A150 080

*EXPERIMENTAL STUDIES OF QUASI-TWO-DIMENSIONAL  
AND THREE-DIMENSIONAL VISCOUS INTERACTION  
REGIONS INDUCED BY SKEWED-SHOCK AND SWEPT-SHOCK  
BOUNDARY LAYER INTERACTIONS*

**FINAL TECHNICAL REPORT**

Calspan Report No. 7018-A-2  
July 1984

**TECHNICAL REPORT**

GTB 100% COPY

DTIC  
SELECTED  
JAN 22 1985  
S D  
B

ARVIN CALSPAN ADVANCED TECHNOLOGY CENTER

PO BOX 400 BUFFALO NEW YORK 14225

85 01 14 012

Approved for public release;  
distribution unlimited.

# **ARVIN/CALSPAN**

**EXPERIMENTAL STUDIES OF QUASI-TWO-DIMENSIONAL  
AND THREE-DIMENSIONAL VISCOUS INTERACTION  
REGIONS INDUCED BY SKEWED-SHOCK AND SWEPT-SHOCK  
BOUNDARY LAYER INTERACTIONS**

**FINAL TECHNICAL REPORT**

**Calspan Report No. 7018-A-2  
July 1984**

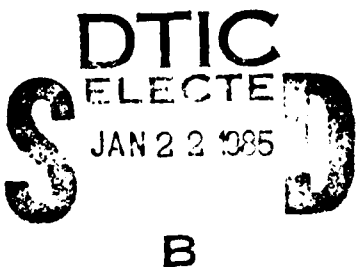
**Contract No. F49620-82-C-0026**

**Prepared for:**

**AIR FORCE OFFICE OF SCIENTIFIC RESEARCH  
BOLLING AIR FORCE BASE, D.C. 20332**

**Principal Investigator:**

**Michael S. Holden  
Physical Sciences Department**



ADVANCED TECHNOLOGY CENTER PO BOX 400 BUFFALO, NEW YORK 14225

Cable CALSPAN Telex 91-270 TEL (716) 632-7500

**DISTRIBUTION STATEMENT A**  
Approved for public release  
Distribution Unlimited

## UNCLASSIFIED

SECURITY CLASSIFICATION OF THIS PAGE

## REPORT DOCUMENTATION PAGE

1a. REPORT SECURITY CLASSIFICATION Unclassified		1b. RESTRICTIVE MARKINGS			
2a. SECURITY CLASSIFICATION AUTHORITY		3. DISTRIBUTION/AVAILABILITY OF REPORT Approved for Public Release; Distribution Unlimited			
2b. DECLASSIFICATION/DOWNGRADING SCHEDULE					
4. PERFORMING ORGANIZATION REPORT NUMBER(S)  7018-A-2		5. MONITORING ORGANIZATION REPORT NUMBER(S)  AFOSR-TR-82-28			
6a. NAME OF PERFORMING ORGANIZATION Calspan Advanced Technology Center	6b. OFFICE SYMBOL (if applicable) NA	7a. NAME OF MONITORING ORGANIZATION			
6c. ADDRESS (City, State and ZIP Code) P.O. Box 400 Buffalo, NY 14225		7b. ADDRESS (City, State and ZIP Code)			
8a. NAME OF FUNDING/SPONSORING ORGANIZATION Air Force Office of Scientific Research	8b. OFFICE SYMBOL (if applicable) NA	9. PROCUREMENT INSTRUMENT IDENTIFICATION NUMBER F49620-82-C-0026			
8c. ADDRESS (City, State and ZIP Code) Bolling Air Force Base Washington, DC 20332		10. SOURCE OF FUNDING NOS.			
		PROGRAM ELEMENT NO. 61102F	PROJECT NO. 2307	TASK NO. A1	WORK UNIT NO.
11. TITLE (Include Security Classification) (See attached sheet)					
12. PERSONAL AUTHOR(S) Michael S. Holden					
13a. TYPE OF REPORT Final	13b. TIME COVERED FROM 1/15/82 TO 7/31/84	14. DATE OF REPORT (Yr., Mo., Day) July 1984		15. PAGE COUNT 74	
16. SUPPLEMENTARY NOTATION					
17. COSATI CODES		18. SUBJECT TERMS (Continue on reverse if necessary and identify by block number) Shock Wave/Boundary Layer Interaction 3D Viscous/Inviscid Interaction Hypersonic, High Reynolds Number Turbulent Flow Corner Interaction Cone-Flare			
19. ABSTRACT (Continue on reverse if necessary and identify by block number) This report describes the results from three experimental studies designed to examine the aerothermal characteristics of regions of three-dimensional shock wave/boundary layer interaction in high-speed flow over non-adiabatic surfaces. The objective of these studies was to explore the basic mechanisms associated with three-dimensional boundary layer separation in high-speed flows with special emphasis on the large heat transfer rates and gradients developed in the separation and reattachment regions of these flows. We also wished to obtain detailed sets of experimental measurements with which to extend the simple semi-empirical prediction models to the hypersonic/cooled wall regime where no previous data existed, as well as provide measurements which we hope to compare later with solutions to the Navier-Stokes equations. These studies were conducted at Mach 11 for Reynolds number of up to $40 \times 10^6$ in Calspan's 96-Inch Shock Tunnel. In the first study we examined the effects of crossflow on the scale and properties of attached and separated regions induced over a flat plate at the base of skewed/oblique shocks. Analysis of the detailed heat transfer and pressure measurements together with flow visualizations demonstrated that, for sweep angles of up to 45°, cross flow had little effect on the size or characteristics of the interaction regions. In the second study the swept-shock was induced normal to the flat plate boundary layer by a shock generator mounted perpendicular to the flat plate. This contrasts with the findings of Settles et al, whose measurements indicate that the size of the interaction over a swept wedge increases with increased sweep. Measurements of the distribution of heat transfer and pressure were made on three streamwise rays for a range of					
(cont.)					
20. DISTRIBUTION/AVAILABILITY OF ABSTRACT UNCLASSIFIED/UNLIMITED <input checked="" type="checkbox"/> SAME AS RPT. <input checked="" type="checkbox"/> OTIC USERS <input type="checkbox"/>		21. ABSTRACT SECURITY CLASSIFICATION Unclassified			
22a. NAME OF RESPONSIBLE INDIVIDUAL James D. Wilson, Program Manager		22b. TELEPHONE NUMBER (Include Area Code)		22c. OFFICE SYMBOL	

**UNCLASSIFIED**

SECURITY CLASSIFICATION OF THIS PAGE

**11. TITLE**

Experimental Studies of Quasi-Two Dimensional and Three-Dimensional Viscous Interaction Regions Induced by Skewed-Shock and Swept-Shock Boundary Layer Interactions

**18. SUBJECT TERMS (cont.)**

Skewed Shock Interaction  
3D Separation, Heat Transfer, Pressure

Reattachment Heating, Cross Flow Effects  
in Separated Flow, Shock Tunnel Studies

**19. ABSTRACT (Cont.)**

locations and incidences of the shock generator. Our corner flow measurements demonstrated that in highly-cooled hypersonic flows, the pressure rise to induce incipient separation is significantly larger than predicted by the semi-empirical methods. Measurements of the plateau and peak pressure as well as the maximum heating were correlated with earlier measurements at lower speeds and were in good agreement with simple prediction techniques. In the third investigation a preliminary study was made of the flow field and distribution of properties in the turbulent interaction over a cone-flare compression surface at zero degrees and small angles of incidence. The very large models ( $L = 10$  ft) constructed for these studies resulted in interaction regions of sufficient thickness to allow probing of the separating sublayer. Measurements of the distribution of properties through the turbulent interaction regions were made for local Mach numbers from 8 to 12, for Reynolds numbers from  $10^6$  to  $80 \cdot 10^6$ . The interaction regions, particularly those on the leeside of the configuration, were influenced by angle of attack; however, further study is required to determine to what extent crossflow, as opposed to local inviscid flow conditions, are responsible for such effects.

Accession For	
NTIS GRA&I	<input checked="" type="checkbox"/>
DTIC TAB	<input type="checkbox"/>
Unsue Used	<input type="checkbox"/>
Junk	<input type="checkbox"/>
By _____	
Distribution / _____	
Availability Codes	
Dist	AVAIL AND/or Special
A-1	

**UNCLASSIFIED**

SECURITY CLASSIFICATION OF THIS PAGE

## Abstract

This report describes the results from three experimental studies designed to examine the aerothermal characteristics of regions of three-dimensional shock wave/boundary layer interaction in high-speed flow over non-adiabatic surfaces. The objective of these studies was to explore the basic mechanisms associated with three-dimensional boundary layer separation in high-speed flows with special emphasis on the large heat transfer rates and gradients developed in the separation and reattachment regions of these flows. We also wished to obtain detailed sets of experimental measurements with which to extend the simple semi-empirical prediction methods to the hypersonic/cooled wall regime where no previous data existed, as well as provide measurements which we hope to compare later with solutions to the Navier-Stokes equations. These studies were conducted at Mach 11 for Reynolds number of up to  $40 \times 10^6$  in Calspan's 96-Inch Shock Tunnel. In the first study we examined the effects of crossflow on the scale and properties of attached and separated regions induced over a flat plate at the base of skewed/oblique shocks. Analysis of the detailed heat transfer and pressure measurements together with flow visualizations demonstrated that, for sweep angles of up to  $45^\circ$ , crossflow had little effect on the size or characteristics of the interaction regions. In the second study the swept-shock was induced normal to the flat plate boundary layer by a shock generator mounted perpendicular to the flat plate. This contrasts with the findings of Settles et al, whose measurements indicate that the size of the interaction over a swept wedge increases with increased sweep. Measurements of the distribution of heat transfer and pressure were made on three streamwise rays for a range of locations and incidences of the shock generator. Our corner flow measurements demonstrated that, in highly-cooled hypersonic flows, the pressure rise to induce incipient separation is significantly larger than predicted by the semi-empirical methods. Measurements of the plateau and peak pressure as well as the maximum heating were correlated with earlier measurements at lower speeds and were in good agreement with simple prediction techniques. In the third investigation a preliminary study was made of the flow field and distribution of properties in the turbulent interaction over a cone-flare compression surface at zero degrees and small angles of incidence. The very large models ( $L=10$  ft) constructed for these studies resulted in interaction regions of sufficient thickness to allow probing of the separating sublayer. Measurements of the distribution of properties through the turbulent interaction regions were made for local Mach numbers from 8 to 12, for Reynolds numbers from  $10 \times 10^6$  to  $80 \times 10^6$ . The interaction regions, particularly those on the

leeside of the configuration, were influenced by angle of attack; however, further study is required to determine to what extent crossflow, as opposed to local inviscid flow conditions, are responsible for such effects.

## TABLE OF CONTENTS

<u>Section</u>	<u>Title</u>	<u>Page</u>
I	BACKGROUND	1
II	PROGRAM OBJECTIVES	6
III	EXPERIMENTAL CONDITIONS, MODELS AND INSTRUMENTATION	7
	o Test Conditions and Model Configurations	7
	o Heat Transfer Instrumentation	7
	o Pressure Instrumentation	10
	o Finite Span Effects	10
IV	RESULTS AND DISCUSSION	11
	o Skewed-Oblique-Shock/Turbulent Boundary Layer Interaction Studies	11
	o Discussion of Results	11
	o Sharp-Fin-Induced 3D Corner Interaction Studies	27
	o Discussion of Results	27
	o Studies of Shock-Wave/Turbulent Boundary Layer Interaction at a Cone/Flare Junction	30
	CONCLUSIONS	63
	REFERENCES	65

## LIST OF ILLUSTRATIONS

<u>Number</u>	<u>Title</u>	<u>Page</u>
1	Typical Surface Heating and Surface Pressure Distributions Through Swept Shock/Turbulent Boundary Layer Interaction	4
2a	Schematic Diagram of Skewed-Oblique-Shock/Boundary Layer Interaction Configuration	8
2b	Schematic Diagram of Swept-Shock/Interaction Configuration	8
3	Swept-Oblique-Shock Interaction Model	12
4	Streamwise Distributions of Heat Transfer and Pressure Through Skewed-Oblique-Shock Boundary Layer Interaction ( $\theta = 12.5^\circ$ $\psi = 0^\circ$ )	13
5	Streamwise Distributions of Heat Transfer and Pressure Through Skewed-Oblique-Shock Boundary Layer Interaction ( $\theta = 15^\circ$ $\psi = 0^\circ$ )	14
6a	Streamwise Distribution of Heat Transfer and Pressure Through Skewed-Oblique-Shock Interaction ( $\theta = 15^\circ$ $\psi = 15^\circ$ )	16
6b	Streamwise Distribution of Heat Transfer and Pressure Through Skewed-Oblique-Shock Interaction ( $\theta = 15^\circ$ $\psi = 30^\circ$ )	17
6c	Streamwise Distribution of Heat Transfer and Pressure Through Skewed-Oblique-Shock Interaction ( $\theta = 15^\circ$ $\psi = 30^\circ$ )	18
7a	Comparison Between Pressure Distributions Through Skewed-Oblique-Shock Interactions of the Same Strength For a Range of Angles	19
7b	Comparison Between Heat Transfer Distributions Through Skewed-Oblique-Shock Interactions of the Same Strength For a Range of Sweep Angles	19
8a	Streamwise Distribution of Heat Transfer and Pressure Through a Skewed-Oblique-Shock Interaction Region ( $\theta = 12.5^\circ$ $\psi = 15^\circ$ )	20
8b	Streamwise Distribution of Heat Transfer and Pressure Through a Skewed-Oblique-Shock Interaction Region ( $\theta = 12.5^\circ$ $\psi = 30^\circ$ )	21
8c	Streamwise Distribution of Heat Transfer and Pressure Through a Skewed-Oblique-Shock Interaction Region ( $\theta = 12.5^\circ$ $\psi = 45^\circ$ )	22
9a	Comparison Between Pressure Distributions Through Skewed-Oblique-Shock Interaction Regions of the Same Strength For a Range of Sweep Angles	23
9b	Comparison Between Heat Transfer Distributions Through Skewed-Oblique-Shock Interaction Regions of the Same Strength For A Range of Sweep Angles	23

LIST OF ILLUSTRATIONS (Cont.)

<u>Figure</u>	<u>Title</u>	<u>Page</u>
10	Variation of Streamwise Extent of Interaction Ahead of Shock Impingement (or Corner) with Sweep Angle	24
11	Correlation of Plateau Pressure Measurements Obtained In 2D and 3D Flows Showing Little Effect of Crossflow on Plateau Pressure	25
12	Correlation of Plateau Heating Ratio With Plateau Pressure Ratio Showing Measurement From Current Study Agrees Well With Earlier 3D Flow Studies	26
13	Schematic Representation of Attached and Separated Regions in Swept-Shock/Boundary Layer Interactions (Ref. 34)	28
14	Corner Interaction Model	29
15	Streamwise Distribution of Heat Transfer and Pressure Through Swept-Shock Interaction ( $\alpha = 5^\circ$ )	31
16	Streamwise Distribution of Heat Transfer and Pressure Through Swept-Shock Interaction ( $\alpha = 6.5^\circ$ )	32
17	Streamwise Distribution of Heat Transfer and Pressure Through Swept-Shock Interaction ( $\alpha = 7.5^\circ$ )	33
18	Streamwise Distribution of Heat Transfer and Pressure Through Swept-Shock Interaction ( $\alpha = 10^\circ$ )	34
19	Streamwise Distribution of Heat Transfer and Pressure Through Swept-Shock Interaction ( $\alpha = 12.5^\circ$ )	34
20	Variation of Pressure Distribution Through Swept-Shock Interaction Regions With Shock Generator Angle	35
21	Variation of Heat Transfer Distribution Through Swept-Shock Interaction Regions With Shock Generator Angle	36
22	Variation of Shock Generator Angle To Induce Incipient Separation With Mach Numbers	37
23	Correlation of Plateau Pressure Measurement From Swept-Shock Interaction Studies	37
24	Location of Beginning of Peak Heating Region	38
25	Correlation of Maximum Heating Rate In Wedge- and Externally-Generated Shock-Induced Turbulent Separated Flows	39

LIST OF ILLUSTRATIONS (Cont.)

<u>Figure</u>	<u>Title</u>	<u>Page</u>
26	Correlation of Peak Heating Rates in Skewed- and Swept-Shock Interaction Regions	40
27	Correlation of Maximum Pressures Recorded in Swept-Shock Interaction Regions	41
28	Schematic Diagram of Large 6° Cone with Flare used in Studies	43
29	Spherical Nosetip Mounted on Large 6° Cone	44
30	Comparison Between Measured Pressure Distribution and Theory For Spherically Capped 6° Cone at 3° Incidence	45
31	Sharp 6° Cone/30° Flare Model Installed in Calspan's 96" Shock Tunnel	47
32a	Distribution of Pressure In Attached Flow Over the Large 6° Cone/30° Flare Configuration	49
32b	Distribution of Heat Transfer In Attached Flow Over the Large 6° Cone/30° Flare Configuration	50
33a	Distribution of Pressure In Separated Flow Over the Large 6° Cone/36° Flare Configuration	51
33b	Distribution of Heat Transfer In Separated Flow Over the Large 6° Cone/36° Flare Configuration	52
34a	Distribution of Pressure In Attached Flow Over the Large 6° Cone/30° Flare Configuration	53
34b	Distribution of Heat Transfer In Attached Flow Over the Large 6° Cone/30° Flare Configuration	54
35a	Distribution of Pressure In Separated Flow Over the Large 6° Cone/36° Flare Configuration	55
35b	Distribution of Heat Transfer In Separated Flow Over the Large 6° Cone/36° Flare Configuration	56
36a	Distribution of Pressure In Attached Flow Over the Large 6° Cone/30° Flare Configuration	57
36b	Distribution of Heat Transfer In Attached Flow Over the Large 6° Cone/30° Flare Configuration	58
37	Wedge Angle To Induce Incipient Separation	59

LIST OF ILLUSTRATIONS (Cont.)

<u>Figure</u>	<u>Title</u>	<u>Page</u>
38	Correlation of Plateau Pressure Measurements on 6° Cone/36° Flare Configuration With Earlier Measurements	60
39	Correlation of Plateau Heating and Pressure Measurements On Cone/Flare Configuration With Earlier Measurements	61
40	Correlation of Peak Heating and Pressure Measurement on Cone/Flare Configuration With Earlier Measurements	62

## LIST OF TABLES

<u>Number</u>	<u>Title</u>	<u>Page</u>
1	Typical Test Conditions	9
2	Test Conditions for the Cone/Flare Study	46

## I. Background

The large aerothermal loads and severe flow distortions which are generated in three-dimensional regions of shock-wave/turbulent boundary layer interaction are of serious concern to the designers of hypersonic vehicles. In such interactions, which can occur at fin/wing-body junctions, engine inlets, and between aerodynamic components, heating levels as much as five times those generated in stagnation regions can be developed. The size and distribution of properties through these regions are not easily predicted, even with the most sophisticated computational techniques. It is generally recognized that the calculation of a three-dimensional region of turbulent separated flow induced by shock-wave/boundary layer interaction represents one of the most severe tests for the numerical prediction techniques. The difficulty in modeling these flows results, in part, from the very large pressure and heat transfer gradients which are generated in both the streamwise and transverse planes through the interaction regions. In particular, the modeling of turbulence and the selection of the grid geometry in such regions is not a simple matter.

During the past two decades, significant efforts have been devoted to the experimental and theoretical study of attached and separated flows in regions of viscous/inviscid interaction. Initially, the major objective of these programs was to generate physical insight into the basic fluid mechanical mechanisms involved in such interaction regions enabling relatively simple analytical models to be constructed. More recently, with the development of large computers on which to solve the Navier-Stokes equations, the emphasis has switched to modeling the macroscopic features of the flow, namely, turbulence.

Early investigations of shock wave/boundary layer interaction were centered around studies of two-dimensional interaction regions, principally because the conceptual modeling of two-dimensional boundary layer separation is clearly simpler than its three-dimensional counterpart. Initial emphasis was placed on understanding the mechanism upstream in the boundary layer, and the mutual and self-sustaining interaction between the viscous and inviscid flow that, at least in laminar flows, is a key mechanism in separation and reattachment regions. Following the fundamental studies of Howarth<sup>1</sup>, Oswatitsch<sup>2</sup> and Lighthill<sup>3</sup>, Crocco & Lees<sup>4</sup> developed the first technique to calculate the separation of a laminar boundary layer using a "free interaction model" to describe the self-induced interaction between the viscous and inviscid flow. Glick<sup>5</sup> and Bray et

al<sup>6</sup> further refined this model, however, by adding the moment-of-momentum equation. Honda<sup>7</sup> and later Lees and Reeves<sup>8</sup> removed the empiricism of the earlier formulations to obtain integral solutions which successfully described the general features of regions of shock wave/laminar boundary interaction observed in experiments in supersonic flows over adiabatic walls. Later Holden<sup>9</sup> added the integral form of the energy equation to those of mass, momentum, and moment-of-momentum employed by Honda to describe separated interaction regions with heat transfer. In high Mach number flows, Holden<sup>10</sup> also found it necessary to add the normal momentum equation to account for the normal pressure gradient through the boundary layer in the separation and reattachment regions. While laminar interaction problems have yielded to relatively simple prediction techniques, efforts to employ similar methods to describe shock wave/turbulent boundary layer interactions in high-speed flows have met with limited success. This we believe is because the basic interaction mechanisms in the separation of laminar and turbulent boundary layers are fundamentally different. Employing conventional boundary layer techniques to describe turbulent boundary layer separation in high-speed flows may be a serious error.

Many of the conceptual problems associated with the use of the boundary layer equations to describe separated regions induced by shock wave/turbulent boundary layer interaction are circumvented by the direct solution of the Navier-Stokes equations. However, in their place we find the equally thorny problem of specifying a detailed model of turbulence for flows with exceedingly large streamwise pressure gradients. Despite the lack of success in developing credible turbulence models for two-dimensional interaction regions, or perhaps because of it, three-dimensional turbulent interaction regions have become the focus of attention of the Navier-Stokes solvers.

The axial corner flow or swept-shock interaction has been one of the principal configurations selected to investigate three-dimensional regions of shock wave/boundary layer interaction. The swept-shock, which is generated by a wedge or fin mounted perpendicular to a flat plate, impinges normally onto the flat plate boundary layer. The initial studies in this area by Stalker<sup>11</sup> and Stanbrook<sup>12</sup> were followed by the more detailed investigations of McCabe<sup>13</sup>, Peake and Rainbird<sup>14</sup>, Oskam et al<sup>15</sup>, Cousteix and Houdeville<sup>16</sup>, Dolling and Bogdonoff<sup>17,18</sup>, Dolling and Murphy<sup>19</sup>, and Dolling<sup>20</sup>. The latter extensive series of studies were conducted at Mach 3 under adiabatic wall conditions. While incipient separation is relatively easy to define for two-dimensional turbulent interactions, this concept has generated considerable

controversy in three-dimensional flows. While McCabe<sup>13</sup> suggests that separation should be defined on the basis of converging streamlines, Stanbrook<sup>12</sup> and others have used criteria based on the inflection points in the pressure distribution. The occurrence of separation was correlated in simple terms by Korkegi<sup>21</sup>, who found that in low Mach number flow, deflection angle  $\theta_{wi}$  for incipient separation varies as the inverse of the upstream Mach number, i.e.,  $\theta_{wi} = 0.3/M_\infty$ , while for  $2 < M < 3.4$  Korkegi suggests that  $\pi_i/\pi$  is independent of Mach number. Goldberg's<sup>22</sup> measurements at Mach 6 do not agree with the Korkegi correlation.

Studies with the emphasis on the heating in swept-shock interaction regions have been conducted by Neumann and Burke<sup>23</sup>, Goldberg<sup>22</sup>, Token<sup>24</sup>, and Scuderi<sup>25</sup>. Figure 1 shows typical distributions of heat transfer and pressure along a streamwise cut through the interaction region together with nomenclature which is in conventional use. While the heat transfer and pressure distributions exhibit a uniform and monotonic increase through attached interaction regions, when the flow separates, distinctive plateau regions are formed in the heat transfer and pressure distributions, as depicted in Figure 1. As noted above, at low Mach numbers ( $M = 2 \rightarrow 4$ ) and for adiabatic surfaces, a large body of data exists on the mean characteristics of swept-shock interactions. Strangely, this body of 3D data has been found to be in better overall agreement with the Hung and MacCormack<sup>26</sup>, Horstmann<sup>27</sup>, Shang and Hankey<sup>28</sup>, Settles and Horstmann<sup>29</sup> solutions to the Navier-Stokes equations than the relatively less complex two-dimensional flow separation over a flat plate/wedge. These results are not as sensitive to the turbulence model and suggest that the gross features of the flows are controlled principally by inviscid effects.

Another approach to exploring flow separation in regions of three-dimensional shock wave/boundary layer interaction is to begin with a two-dimensional or axisymmetric interaction and sweep this interaction (or introduce angle of attack for the axisymmetric case) to progressively introduce crossflow into the interaction region. Experimental studies of this type have been conducted by Ericsson, Reding and Guenther<sup>30</sup>, Settles and Perkins<sup>31</sup>, and Settles and Teng<sup>32</sup>. Settles, who studied the interaction region over swept and unswept flat plate/wedge configurations in an adiabatic Mach 3 airflow, found that introducing crossflow increased the scale of the separated interaction region. Considerable effort was expended in this latter study to determine the Reynolds number scaling, and the length from the upstream tip of the wedge for the flow to become quasi-two-dimensional. However, the effect of changing the

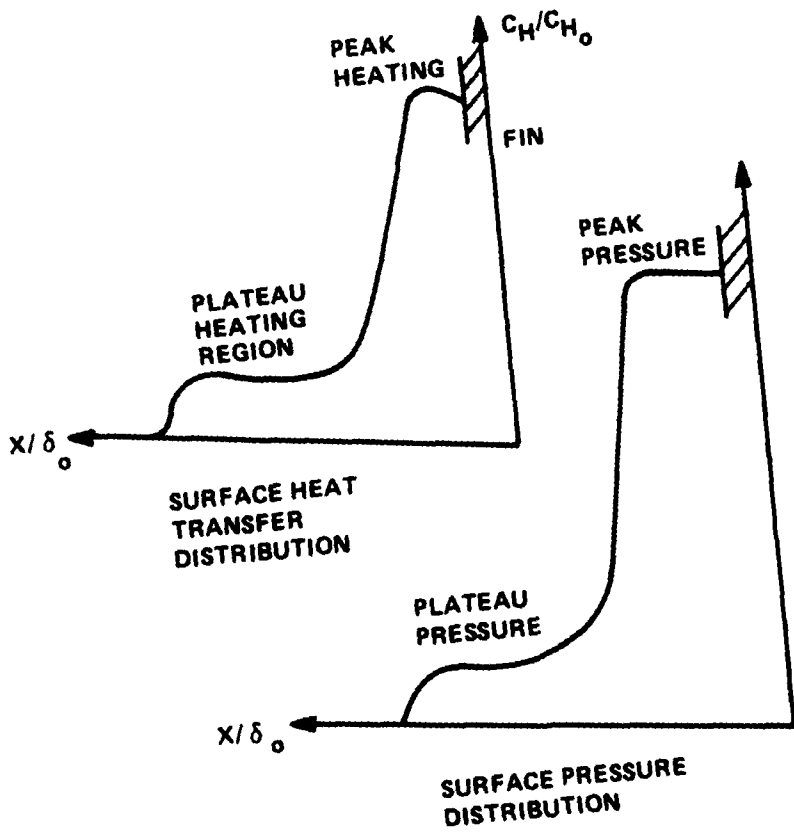
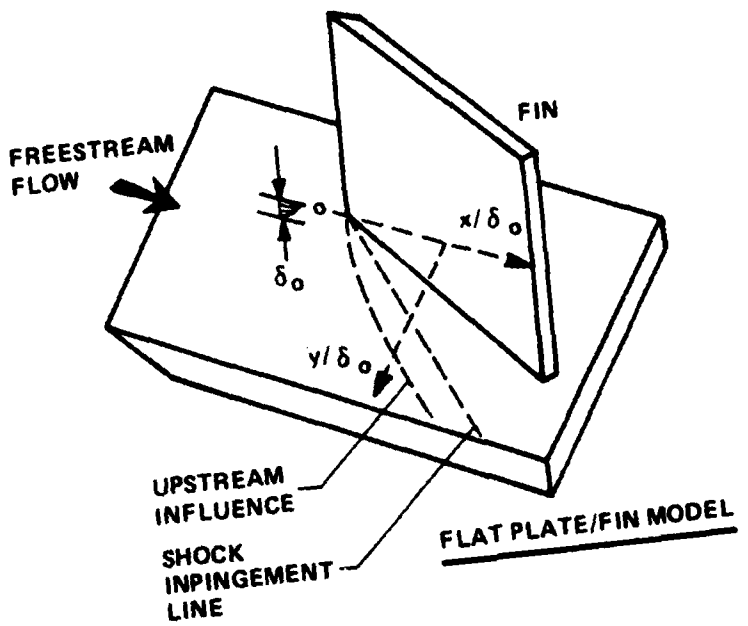


Figure 1 TYPICAL SURFACE HEATING AND SURFACE PRESSURE DISTRIBUTIONS  
THROUGH SWEPT SHOCK/TURBULENT BOUNDARY LAYER INTERACTION

overall spanwise scale of the model on the scale of the interaction was not examined explicitly. The measurements of surface and pitot pressure through the interaction regions were in good agreement with solutions to the Navier-Stokes equations obtained by Horstman<sup>27</sup>; however, some key features of the flow were poorly predicted. It is known that agreement with pressure data is not the most definitive of tests.

Current developments in both computer speed and the design of "fast solvers" for the Navier Stokes equations has led to changes in the requirements for experimental studies, both in the configurations selected for study and the detailed measurements to be made. In general we are less restricted in the selection of a "simple model configuration" as long as the particular boundary conditions are well-defined. However, the measurements made in these studies must be more strongly oriented toward aiding in the selection of the specific mesh geometry and model of turbulence to be used in the numerical description of these flows. An intrinsic problem which faces the experimentalist studying turbulent boundary layer separation in hypersonic flow is that the wall layer, within which separation first occurs and the properties of which are required to define the characteristics of both the attached and separated boundary layer, is very thin--typically five percent of the boundary layer thickness, making the accurate probing of this layer difficult. Thus, to obtain the required resolution, measurements must be made on very large models or on tunnel walls, with miniature but robust instrumentation. As in our earlier studies of two- and three-dimensional shock/boundary layer interaction, we believe that it is useful to perform an experiment in which crossflow can be progressively introduced beginning with a configuration over which the flow is two-dimensional, or axisymmetric. However, as mentioned above, because the measurements made in such a study would be compared with solutions to the Navier-Stokes equations, we can select a model configuration over which the three-dimensional interaction regions are relatively complex, providing the boundary conditions are well defined. Based on these considerations we selected the large cone/flare configuration as the basic model to be used in the third phase of this preliminary study of three-dimensional turbulent viscous/inviscid interaction regions.

The three experimental studies described in this paper were designed to explore the fundamental aerothermal characteristics of attached and separated regions of three-dimensional shock wave/turbulent boundary layer interaction in the high Mach number, high Reynolds number flow regime, where little or no data existed. The two aerodynamic configurations selected for study, the impingement of a swept-shock

generated by a vertical fin onto a flat plate boundary layer, and the interaction between an oblique-skewed-shock and a turbulent boundary layer together provide basic information with which to characterize the heating and pressure distributions in shock-induced 3D interaction regions. In the following sections we first discuss the objective of each study and describe the test conditions, models and instrumentation used in the experimental program. The measurements made in the experimental program are described and discussed, and then the conclusions from this study presented.

## II. Program Objectives

The objective of these studies was to examine the characteristics of attached and separated flow in shock induced 2D and 3D turbulent interaction regions by performing experimental studies in which the geometric configuration of the models were varied, progressively changing the flow from 2D to 3D. We sought to provide information on the quantitative differences between the characteristics of two- and three-dimensional viscous interaction regions, and in particular, examine whether crossflow exerts a strong influence in these flows. An important objective of the current studies was to provide information with which to construct and verify simple prediction techniques, as well as evaluate the turbulence models used in the Navier-Stokes codes.

Two sets of models were used in the swept wing and skewed interaction studies: a model (shown schematically in Figure 2a) which generates the interaction between a swept-oblique and a flat plate boundary layer, and a model (shown schematically in Figure 2b) which generates a swept-normal-shock. In both studies, the model configurations were varied to obtain both two- and three-dimensional flow fields. The model design, the instrumentation, and the test conditions chosen for these studies are described in the following section.

## III. Experimental Conditions, Models and Instrumentation

### Test Conditions and Model Configurations

The experimental studies were conducted in the 96-Inch Shock Tunnel at Calspan, at a Mach number of 11 for Reynolds numbers up to  $50 \times 10^6$ , resulting in  $R_e$ 's just upstream of the interactions of  $2 \times 10^6$  and hence fully turbulent regions

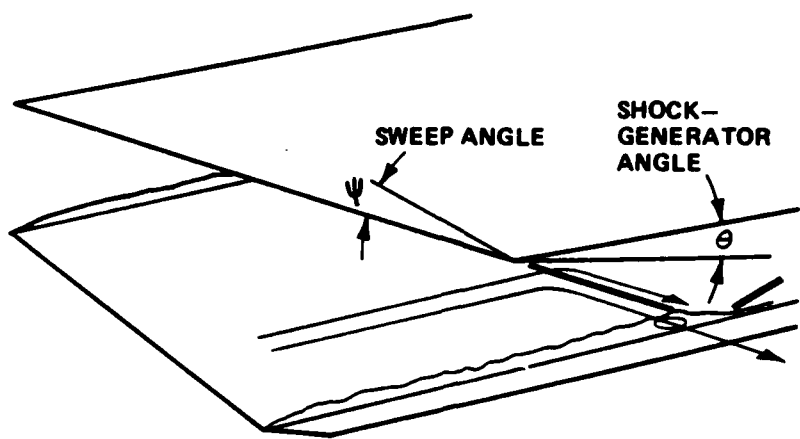


**Figure 2a SCHEMATIC DIAGRAM OF SKEWED-OBLIQUE-SHOCK/BOUNDARY LAYER INTERACTION CONFIGURATION**

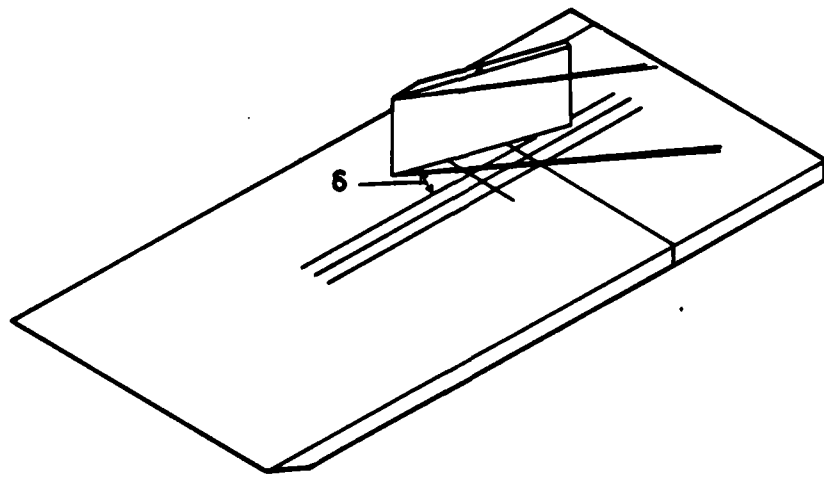


**Figure 2b SCHEMATIC DIAGRAM OF SWEPT-SHOCK/INTERACTION CONFIGURATION**

of shock wave boundary layer interaction. Shock tunnels are in essence blowdown tunnels in which a reservoir of high-pressure, high-temperature air is generated by reflecting a normal shock wave from the end wall of the driven section of the tunnel. The slug of high-temperature compressed air is then expanded through the required nozzle to obtain the desired condition in the test section, for run times between 5 and 20 milliseconds. These run times are orders of magnitude larger than required to establish the flow over the model, and yet are of insufficient duration for destruction of the highly sensitive model instrumentation by the large aerodynamic and heating loads encountered in the tunnel. Table I gives an example of typical test conditions. In the skewed-shock interaction studies, the principal variables were the angle of the shock generator relative to the flat plate and the sweep angle of its leading edge. The position of the leading edge of the shock generator was varied to place the line of shock impingement at the same axial station for each configuration examined. In the sharp-fin-induced, swept-shock boundary layer interaction studies, we varied the incidence of the fin relative to the freestream to change the strength of the interaction, and translated the fin across the plate to place the major rays of instrumentation at various stations along the swept-shock.

#### Heat Transfer Instrumentation

The extremely large heat transfer rates and gradients which are generated in the reattachment regions of shock wave/turbulent boundary interaction in hypersonic flows over cooled walls makes it essential that accurate heat transfer measurements be obtained in experimental studies of these flows. Our earlier studies have demonstrated that heat transfer measurements can also be used as an accurate indication of the occurrence of flow separation and the scale of the separated region. Because of the severe heat transfer gradients developed in these flows, to avoid distortion resulting from transverse heat conduction, it is essential to obtain finely resolved measurements on models constructed with surfaces of poor thermal conductivity. The use of miniature thin film heat transfer instrumentation based on a pyrex substrate, coupled with the relatively small rise in surface temperatures inherent in shock tunnel studies, makes the thin film heat transfer instrumentation almost ideal for this type of study. The high frequency of thin film instrumentation also provides the opportunity to obtain definitive information on the unsteady characteristics of turbulent interaction regions. In these studies we employed platinum thin film gages mounted on pyrex strips such that spatial resolutions of 0.050 inch were obtained in key areas of the flow. Three

**Table 1**  
**TYPICAL TEST CONDITIONS**

M <sub>i</sub>		3.279E+00
P <sub>0</sub>	psia	1.747E+04
H <sub>0</sub>	ft <sup>2</sup> /sec <sup>2</sup>	1.792E+07
T <sub>0</sub>	°R	2.694E+03
M <sub>∞</sub>		1.133E+01
U <sub>∞</sub>	ft/sec	5.876E+03
T <sub>∞</sub>	°R	1.119E+02
P <sub>∞</sub>	psia	2.054E-01
Q <sub>∞</sub>	psia	1.847E+01
RHO <sub>∞</sub>	slugs/ft <sup>3</sup>	1.541E-04
Mu <sub>∞</sub>	slugs/ft·sec	9.410E-08
Re/ft <sub>∞</sub>		9.628E+06
PITOT	psia	3.422E+01

streamwise rows of instrumentation were installed along and to either side of the centerline of the 24 inches wide flat plate.

#### Pressure Instrumentation

We used both flush mounted and orifice pressure gages in these studies to obtain measurements of the mean and fluctuating pressure levels through the interaction regions. Calspan piezoelectric pressure gages were connected to a series of closely spaced orifices to obtain the mean pressure distribution along the plate, while the larger, high frequency, PCB quartz transducers were flush mounted beneath a thin, insulating skin to the surface of the plate in key areas of the flow.

#### Finite Span Effects

Measurements were made to investigate the quasi-two-dimensional nature of the swept/separated interactions, in studies where the shock generator was translated laterally across the flat plate, to obtain configurations in which the edge of the shock generator was as close as 6 inches from the centerline of the flat plate. For this latter configuration, and for the configuration with the shock generator mounted symmetrically above the flat plate, both the centerline heat transfer and the pressure measurements indicated that the flow was independent of the position of the edge of the shock generator, exhibiting two-dimensional and quasi-two-dimensional characteristics respectively for unswept and swept incident shocks.

### IV. Results and Discussion

#### Skewed-Oblique-Shock/Turbulent Boundary Layer

##### Interaction Studies

In these studies we examined the effect of crossflow on the size and properties of regions of shock-wave/ turbulent boundary layer interaction induced by the impingement of a skewed-oblique-shock onto a highly-cooled turbulent boundary layer in high Reynolds number hypersonic flow. The skewed-incident shocks were generated by a shock generator mounted above the flat plate as shown in Figure 3. The leading edge of the shock generator was swept at angles of 0, 15, 30 and 45 degrees from the normal to the freestream flow and rotated about its axis to keep the angle in

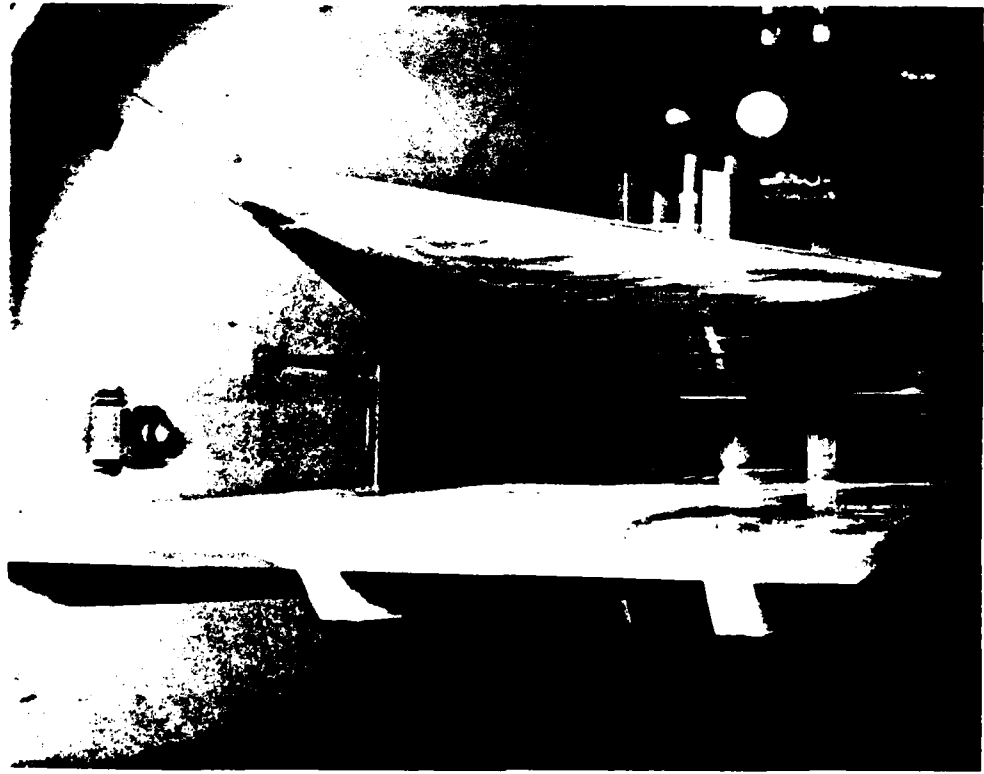
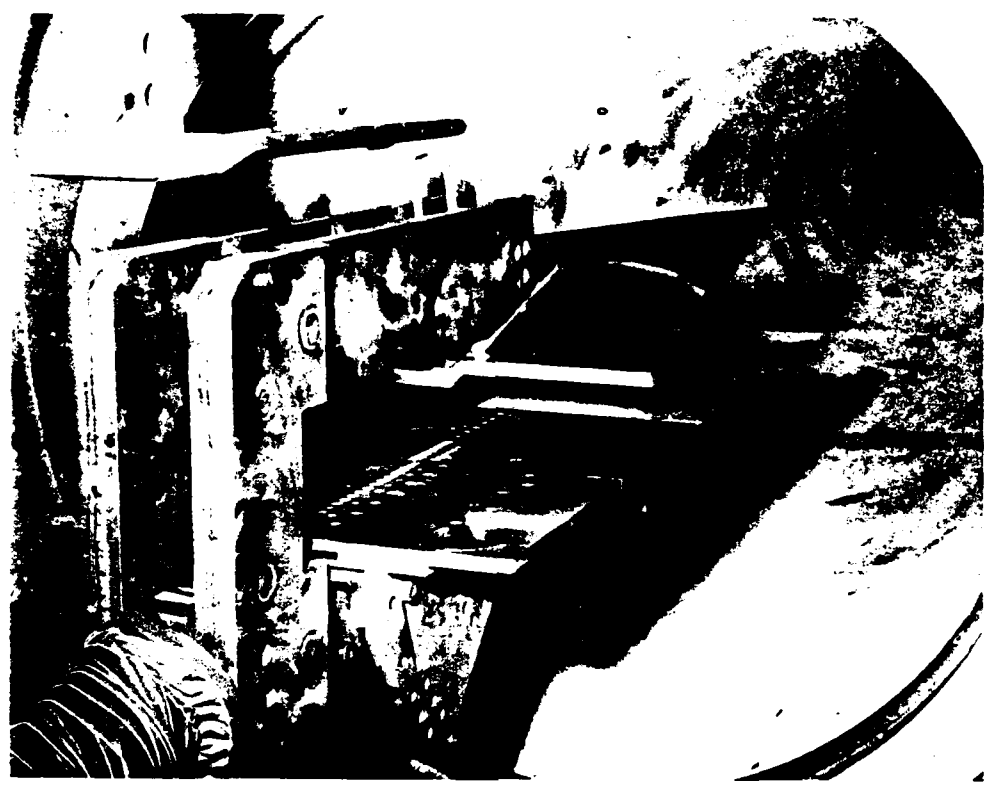


Figure 3 SWEPT-OBLIQUE-SHOCK INTERACTION MODEL

the streamwise plane perpendicular to the flat plate constant. In this way, the strength of the interaction (the overall pressure rise) was held constant and any changes in the size or distribution of properties within the interaction region would reflect the effects of crossflow. It should be observed that to perform studies in hypersonic flow, in which the fully turbulent interaction regions are well defined and uninfluenced by the expansion fan from the trailing edge of the shock generator, the careful design of very large models, the loads on which are on the order of tons, is required. Likewise, the positioning of the incident shocks over the highly instrumented sections of the model and the selection of the gains for the instrumentation, whose outputs varied by three orders of magnitude across the inch-long interaction regions, also represented a challenge.

Discussion of Results. The studies of crossflow effects on the size and properties of the interaction region induced by a swept-oblique-incident on a turbulent boundary layer over a flat plate were conducted for two strengths of incident shock, the first ( $\theta_{SG} = 12.5^\circ$ ) to generate a separated condition close to incipient separation, and the second ( $\theta_{SG} = 15^\circ$ ) to generate a well-separated flow. Distributions of heat transfer and pressure through the interaction regions, as well as schlieren photographs of the unswept or two-dimensional flow condition for each of these shock strengths , are shown in Figures 4 and 5. While the pressure distribution through the weaker interaction shows little evidence of a plateau region, it is clear from the well defined plateau in the heat transfer distribution that a small recirculation region is present. Our earlier studies in which heat transfer, skin friction and pressure measurements were made have confirmed that, in these flows, heat transfer measurements are one of the most sensitive methods for detecting incipient separation. It is clear from the well defined plateau regions in the distributions of pressure and heat transfer, as well as the well defined separation shock in the schlieren photograph, that a well separated region, extending two inches in length, is induced beneath the stronger incident shock.

We anticipated, based on an analogy with the earlier studies of Settles with flat plate/swept wedge configurations at Mach 3, that sweeping the incident shock, while keeping the interaction strength constant, would result in an increase in the streamwise extent of the separated region. In our initial studies, we swept the leading edge by relatively small angles ( $5^\circ$ ); however, it soon became evident that much larger sweep angles were required to induce significant crossflow effects. Consequently the sweep angle was increased in  $15^\circ$  increments to a maximum of  $45^\circ$ . It is clear from

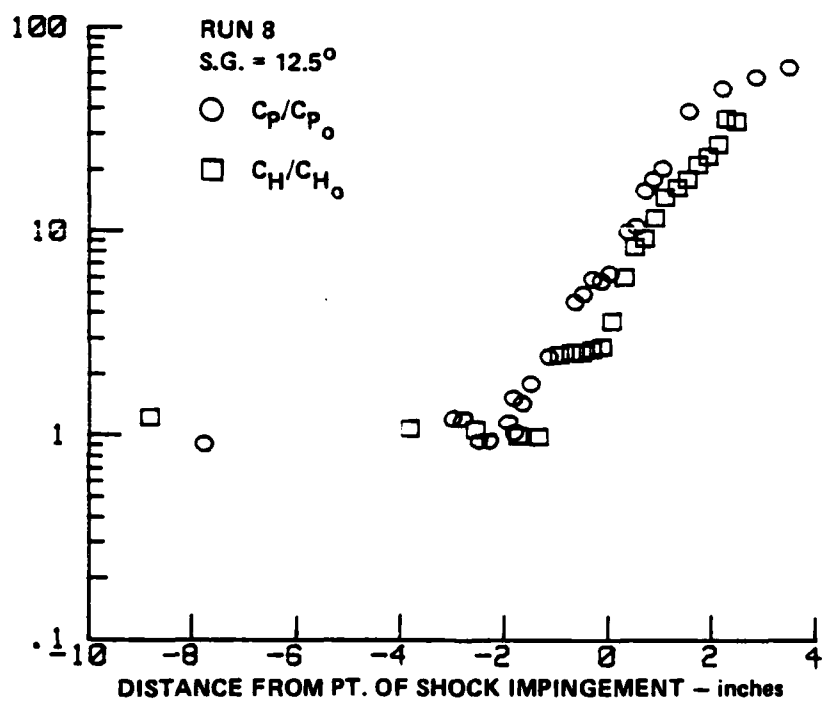


Figure 4 STREAMWISE DISTRIBUTIONS OF HEAT TRANSFER AND PRESSURE THROUGH SKEWED-OBLIQUE-SHOCK BOUNDARY LAYER INTERACTION ( $\theta = 12.5^\circ$   $\psi = 0^\circ$ )

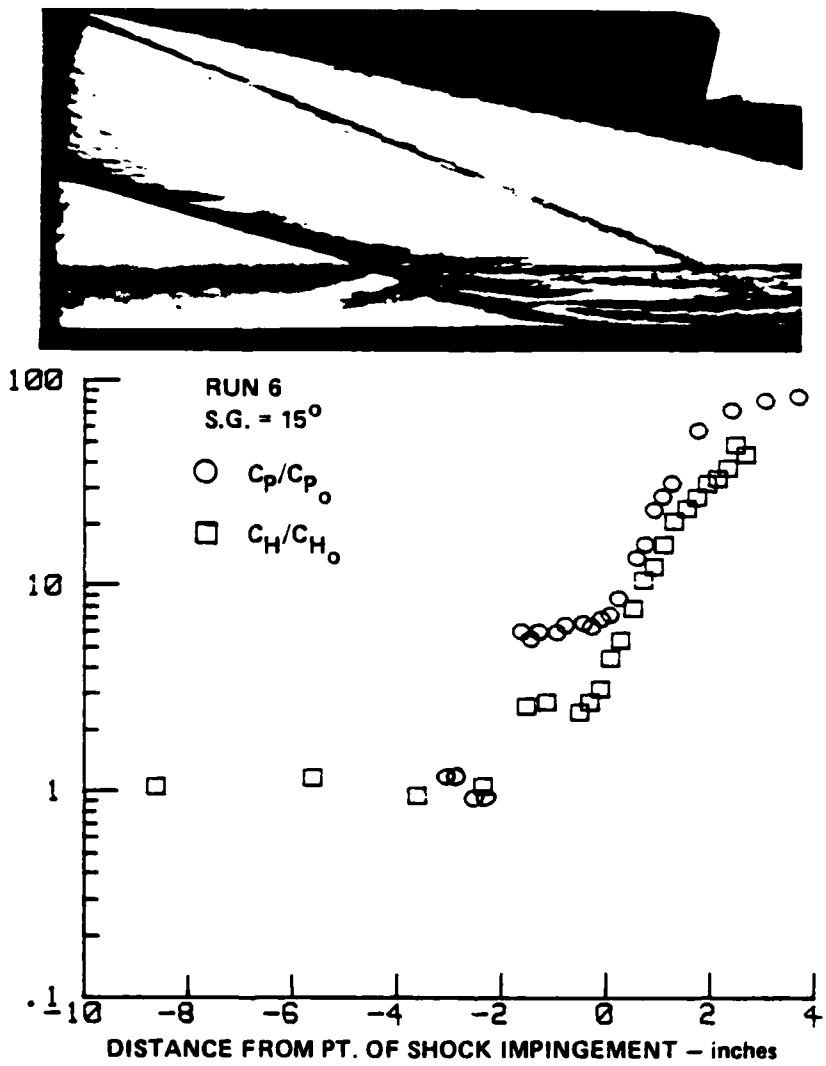


Figure 5 STREAMWISE DISTRIBUTIONS OF HEAT TRANSFER AND PRESSURE  
THROUGH SKEWED-OBLIQUE-SHOCK BOUNDARY LAYER INTERACTION  
( $\theta = 15^\circ$     $\psi = 0^\circ$ )

the measurements made of the distribution of heat transfer and pressure beneath the well separated flow induced by the  $15^\circ$  shock generator swept at angles of 0, 15, 30 and 45 degrees (shown in Figures 6 and 7) that the induced crossflow has little effect on the size and characteristics of the interaction regions. If there is a perceptible effect, it is a decrease in the length of the separated region with increased crossflow. We selected the condition close to incipient separation ( $\theta_{SG} = 12.5^\circ$ ) for study because we believed that this configuration would be one of the most sensitive to crossflow. However, as shown in Figures 8 and 9, sweeping the oblique-shock has little effect on the size or distribution of surface properties through the interaction region. Again, we would assess that any small effect which may have occurred would be in the direction of decreased separation length with increased crossflow. Our measurements across the center span of the model clearly indicated that in Settles terms the interaction was cylindrical (quasi-two-dimensional) for all configurations studied. The significant differences between Settles<sup>29</sup> measurements of the variation of interaction length with sweep angle and those obtained in the current study are shown in Figure 10. While Settles finds an almost threefold increase in separation length at sweep angles of  $40^\circ$ , we find a 10% reduction in this length. In Figures 11 and 12 we compare measurements of plateau pressure and heating made in this study with those obtained in earlier work. Again, we observe little effect of sweep angle on plateau pressure or heating.

#### Sharp-Fin-Induced 3D Corner Interaction

In the corner flow, unlike the flow configuration examined above, the swept-shock generated by the inclined fin impinges on the turbulent boundary layer in a plane perpendicular to the flat plate. The basic mechanism of pressure rise through the interaction is therefore controlled principally by the component of freestream Mach number normal to this shock ( $M_\infty \sin \theta$ ). A highly simplified visualization of the viscous/inviscid interaction with flow separation is sketched in Figure 13. Here, we consider the flow in the plane normal to the plane of the shock to be similar to that in transonic flow. When flow separation occurs, a three-dimensional vortex is formed, the pressure in which is relatively constant at the "two-dimensional" plateau level, as we will show later. The streamwise distribution of heat transfer in this region is also found to be relatively constant, and indeed we and others using skin friction and oil flow measurements have correlated the first appearance of a plateau region in the heat transfer with a significant change in the flow structure which is linked with flow separation. In fact, Token<sup>24</sup> has shown that the McCabe<sup>13</sup> criteria, based on an

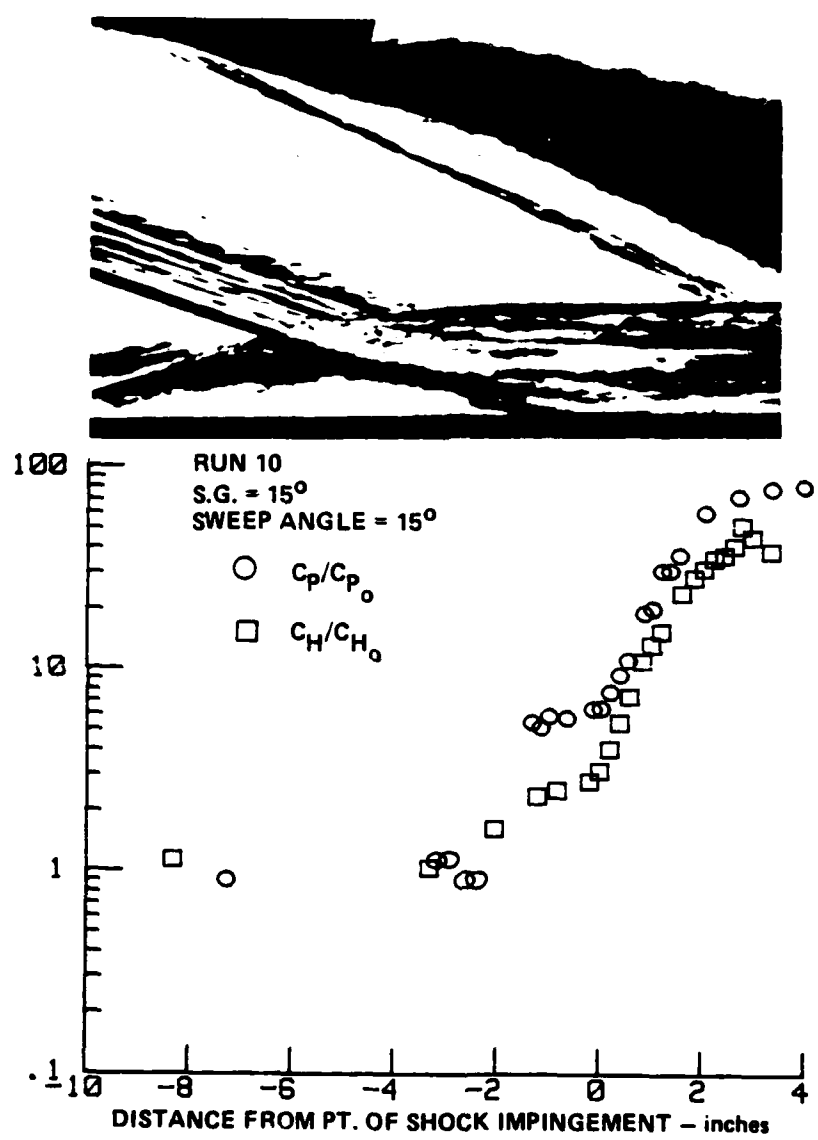


Figure 6a STREAMWISE DISTRIBUTION OF HEAT TRANSFER AND PRESSURE  
THROUGH SKEWED-OBLIQUE-SHOCK INTERACTION ( $\theta = 15^\circ$   $\psi = 15^\circ$ )

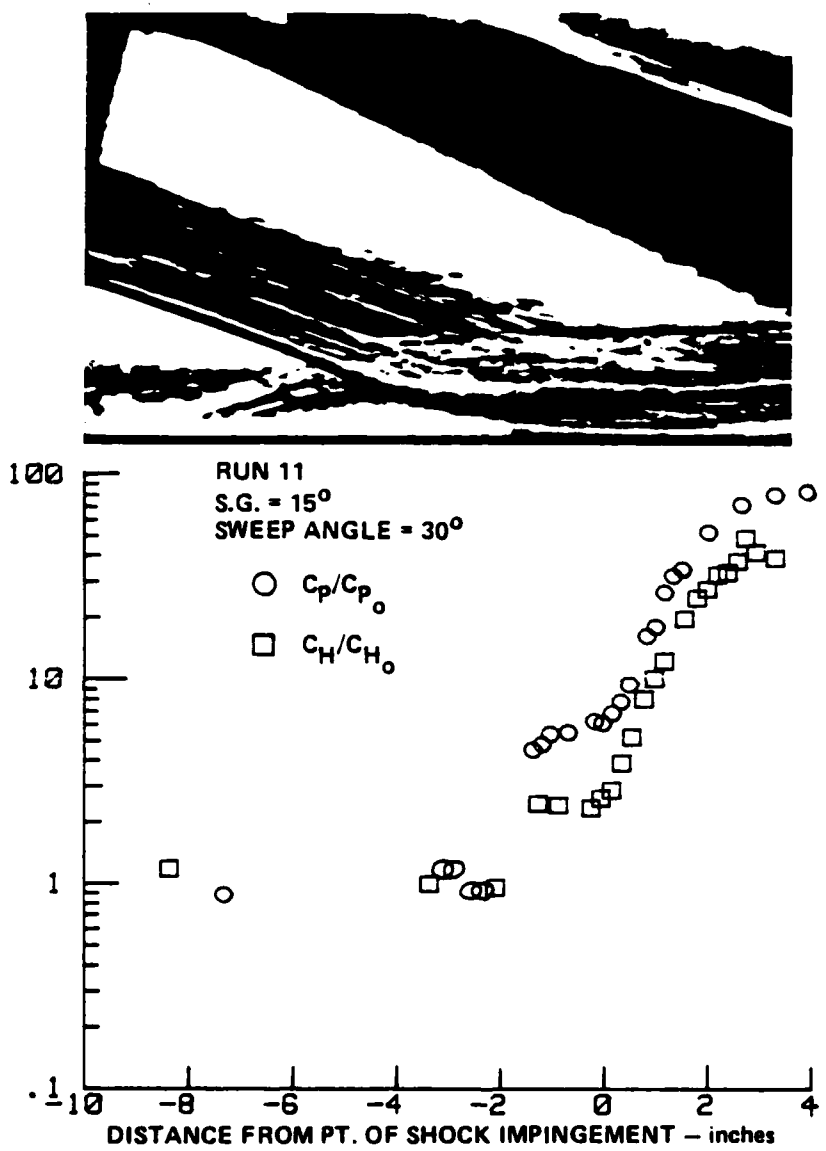


Figure 6b STREAMWISE DISTRIBUTION OF HEAT TRANSFER AND PRESSURE  
THROUGH SKEWED-OBLIQUE-SHOCK INTERACTION ( $\theta = 15^\circ$   $\psi = 30^\circ$ )

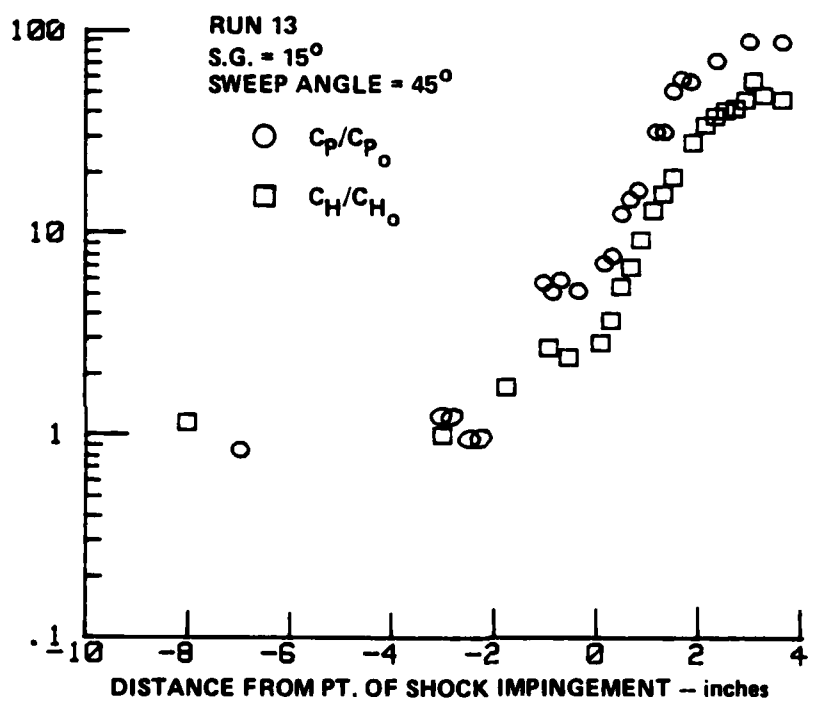
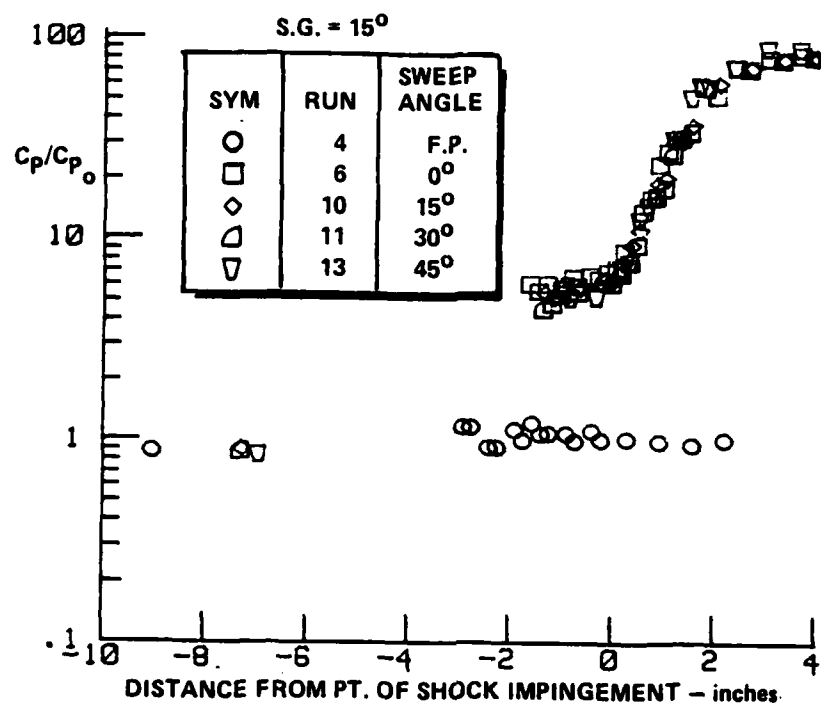
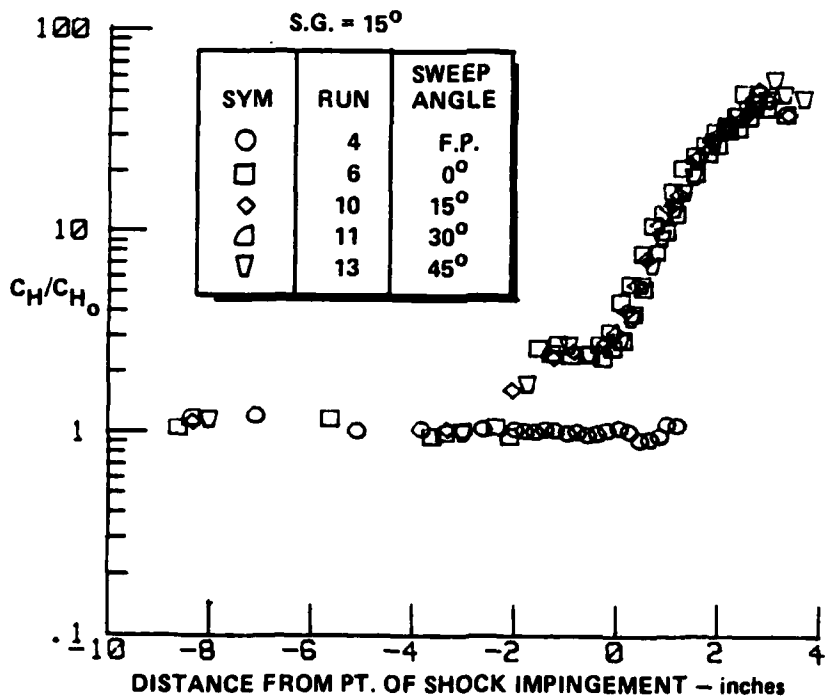


Figure 6c STREAMWISE DISTRIBUTION OF HEAT TRANSFER AND PRESSURE  
THROUGH SKEWED-OBLIQUE-SHOCK INTERACTION ( $\theta = 15^\circ$   $\psi = 30^\circ$ )



**Figure 7a COMPARISON BETWEEN PRESSURE DISTRIBUTIONS THROUGH SKEWED-OBLIQUE-SHOCK INTERACTIONS OF THE SAME STRENGTH FOR A RANGE OF ANGLES**



**Figure 7b COMPARISON BETWEEN HEAT TRANSFER DISTRIBUTIONS THROUGH SKEWED-OBLIQUE-SHOCK INTERACTIONS OF THE SAME STRENGTH FOR A RANGE OF SWEEP ANGLES**

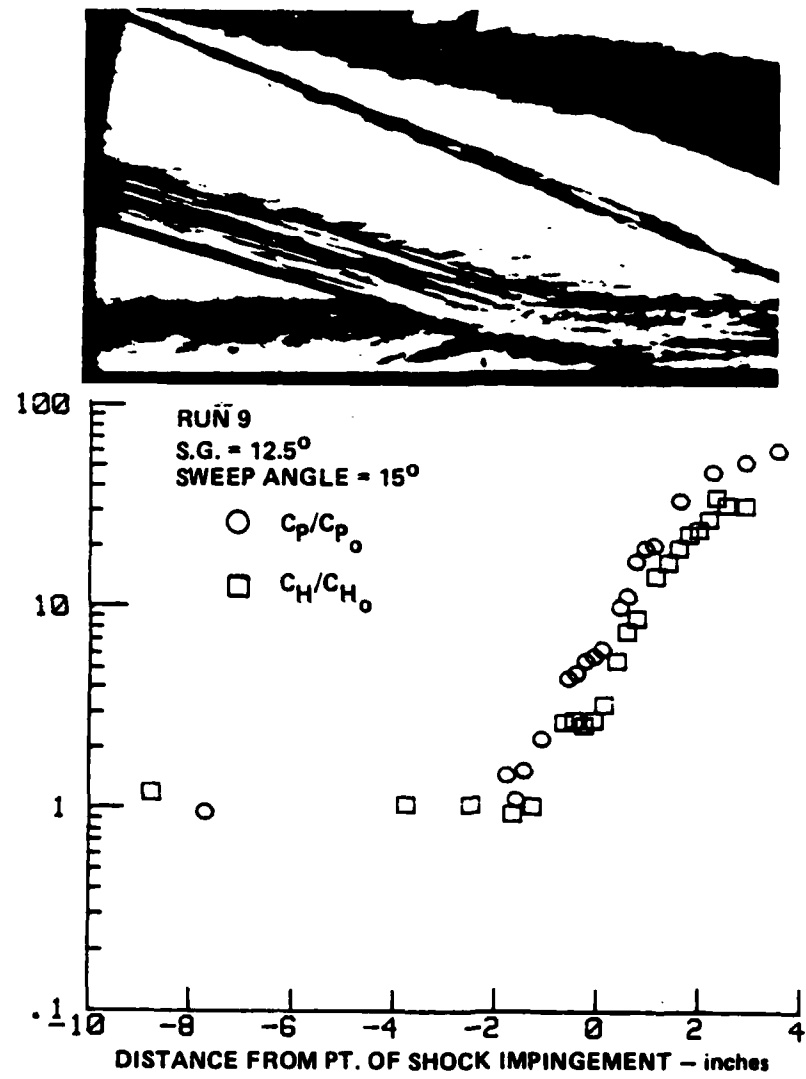


**Figure 8a** STREAMWISE DISTRIBUTION OF HEAT TRANSFER AND PRESSURE  
 THROUGH A SKEWED-OBLIQUE-SHOCK INTERACTION REGION  
 $(\theta = 12.5^{\circ} \quad \psi = 15^{\circ})$

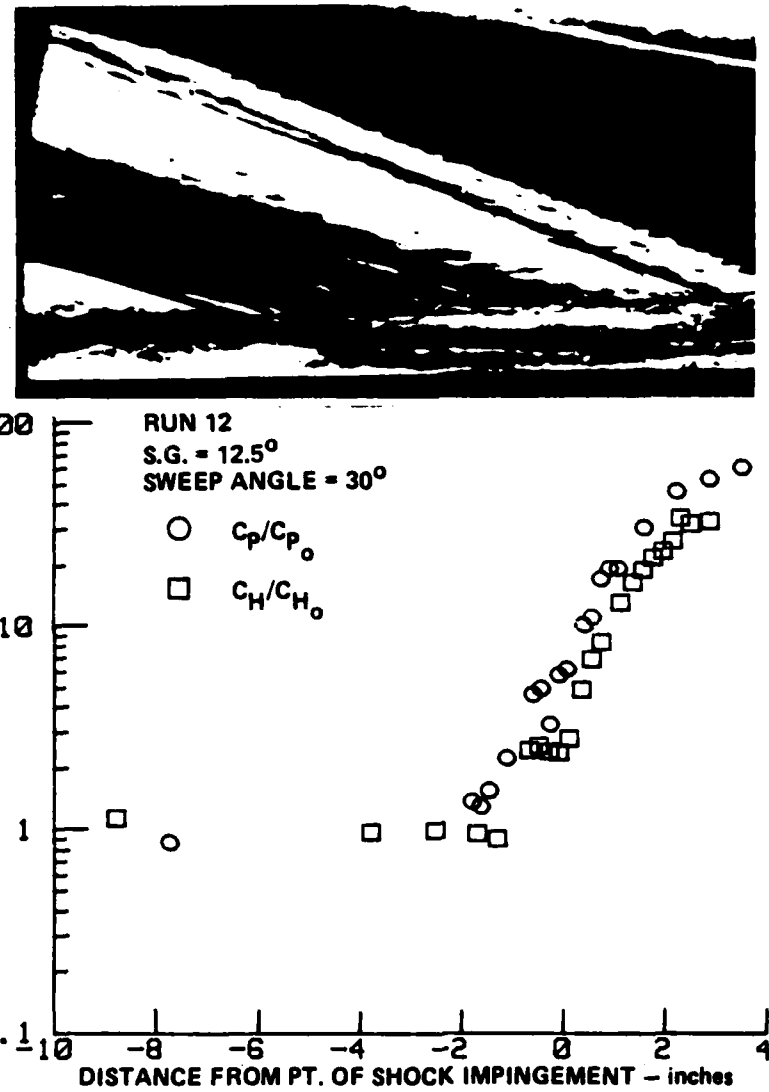


**Figure 8b** STREAMWISE DISTRIBUTION OF HEAT TRANSFER AND PRESSURE  
 THROUGH A SKEWED-OBLIQUE-SHOCK INTERACTION REGION  
 $(\theta = 12.5^\circ \quad \psi = 30^\circ)$

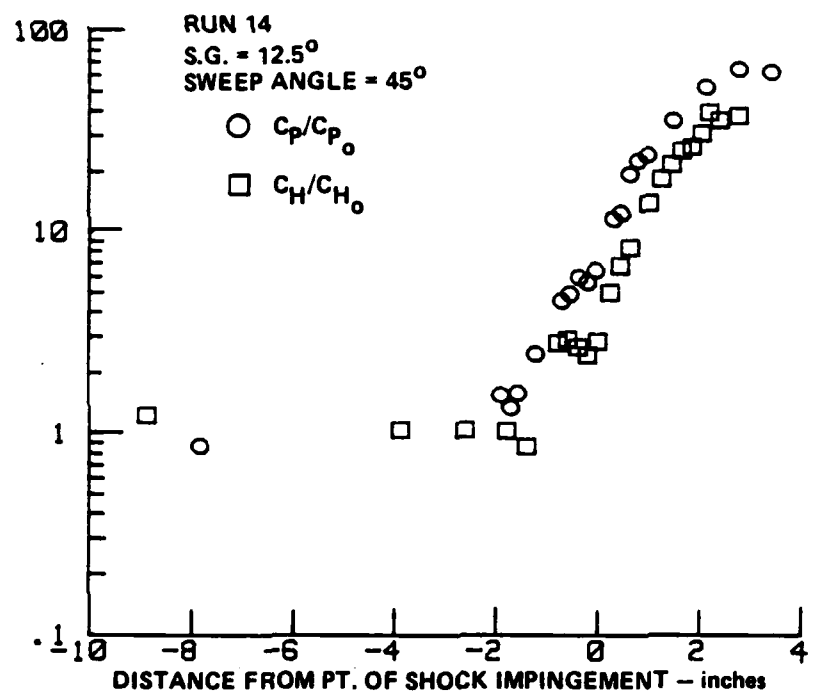
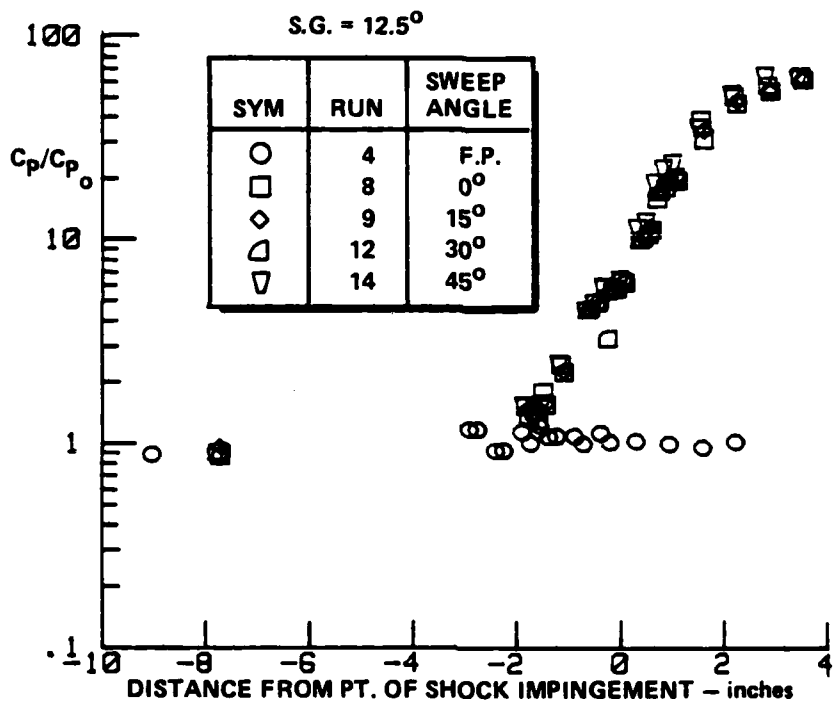
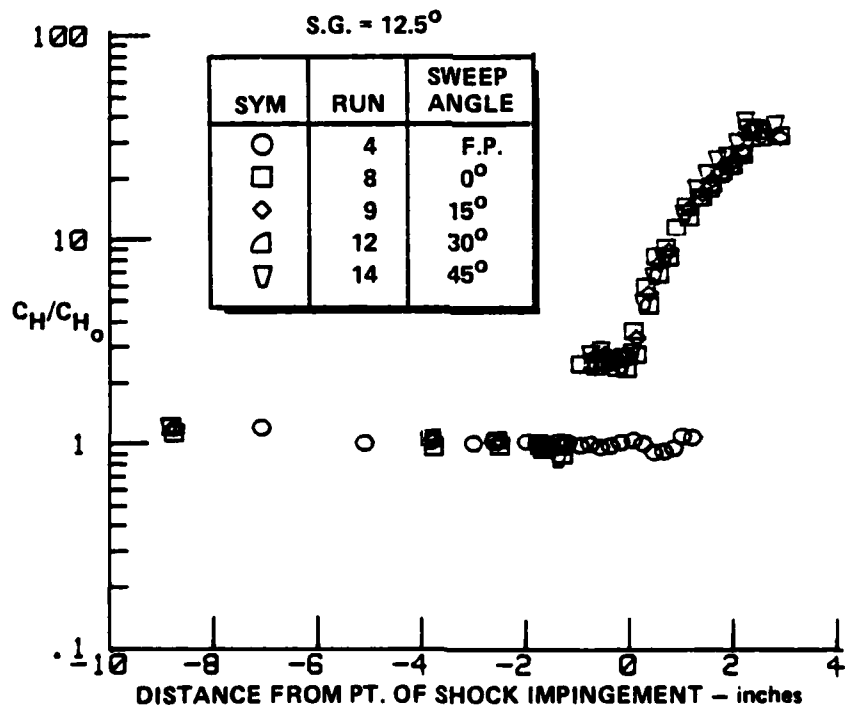


Figure 8c STREAMWISE DISTRIBUTION OF HEAT TRANSFER AND PRESSURE  
THROUGH A SKEWED-OBLIQUE-SHOCK INTERACTION REGION  
( $\theta = 12.5^\circ$   $\psi = 45^\circ$ )



**Figure 9a COMPARISON BETWEEN PRESSURE DISTRIBUTIONS THROUGH SKEWED-OBLIQUE-SHOCK INTERACTIONS OF THE SAME STRENGTH FOR A RANGE OF SWEEP ANGLES**



**Figure 9b COMPARISON BETWEEN HEAT TRANSFER DISTRIBUTIONS THROUGH SKEWED-OBLIQUE-SHOCK INTERACTION REGIONS OF THE SAME STRENGTH FOR A RANGE OF SWEEP ANGLES**

SYM	GEN/WED	SOURCE	$Re_x$
○	16°	SETTLES, PERKINS AND BOGDONOFF ↓ (M = 3)	$18.7 \times 10^6$
□	16°	PRESENT STUDY ↓ (M = 11)	$10.7 \times 10^6$
◇	12.5°		$50 \times 10^6$
□	15°		$50 \times 10^6$

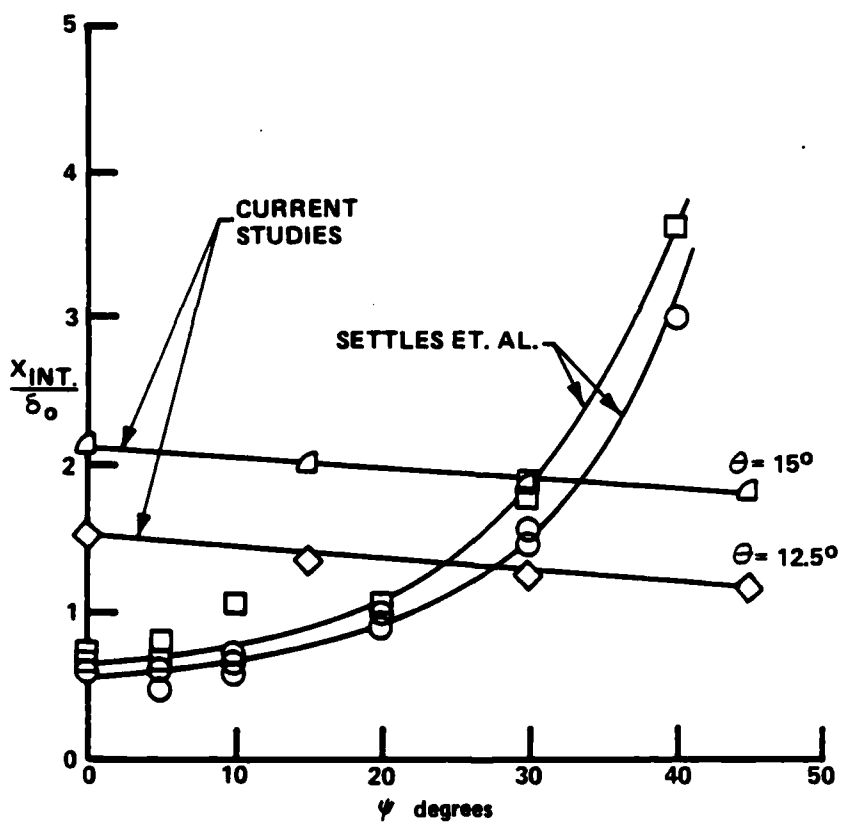


Figure 10 VARIATION OF STREAMWISE EXTENT OF INTERACTION AHEAD OF SHOCK IMPINGEMENT (OR CORNER) WITH SWEEP ANGLE

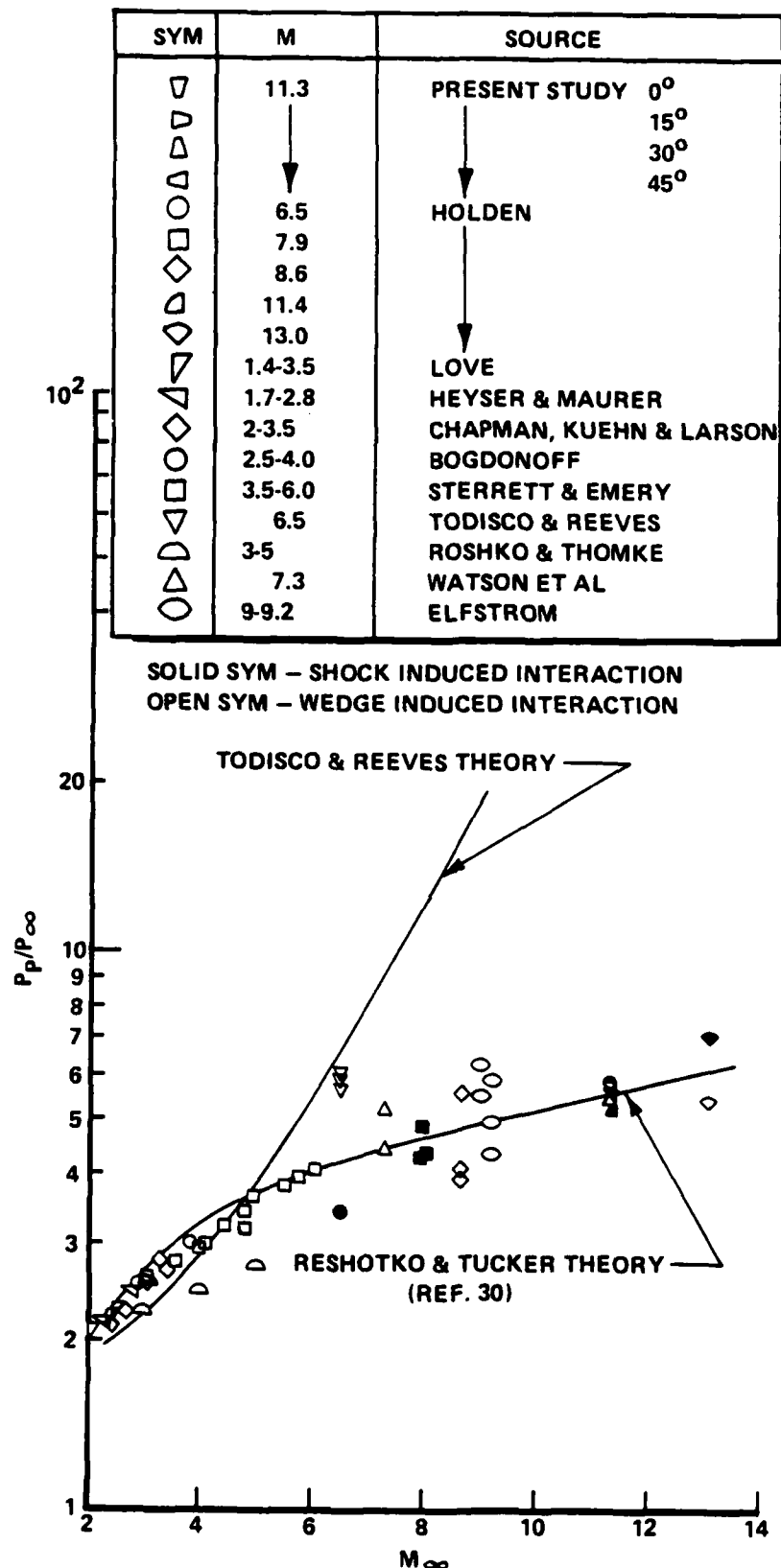


Figure 11 CORRELATION OF PLATEAU PRESSURE MEASUREMENTS OBTAINED IN 2D AND 3D FLOWS SHOWING LITTLE EFFECT OF CROSSFLOW ON PLATEAU PRESSURE

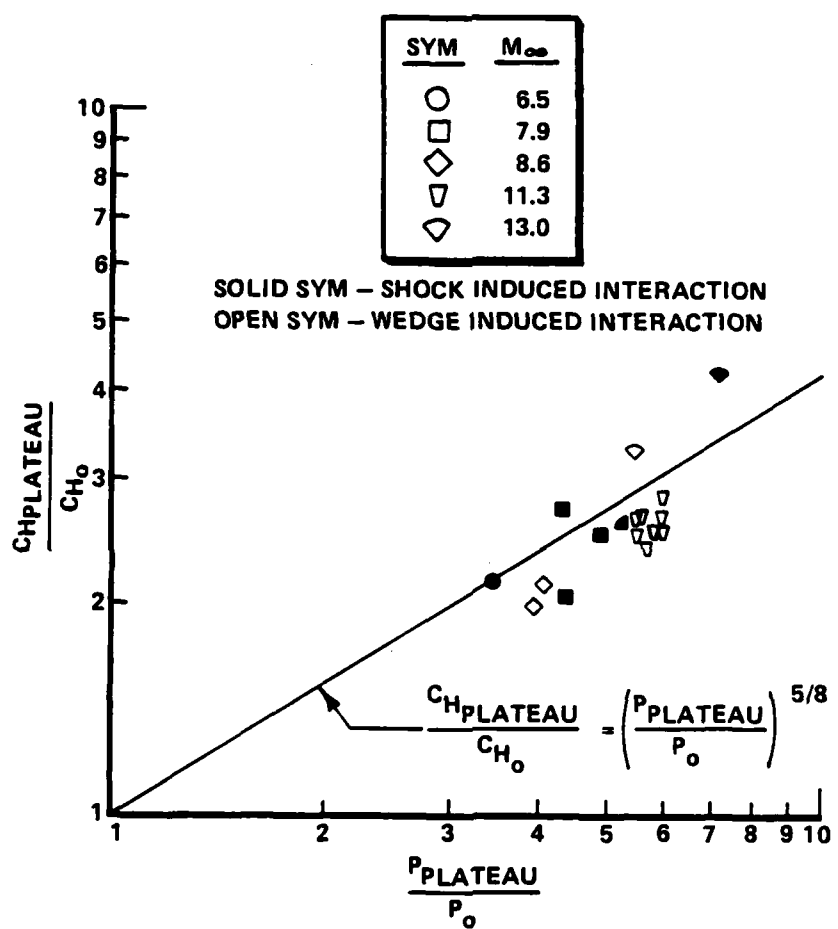


Figure 12 CORRELATION OF PLATEAU HEATING RATIO WITH PLATEAU PRESSURE RATIO SHOWING MEASUREMENT FROM CURRENT STUDY AGREES WELL WITH EARLIER 2D FLOW STUDIES

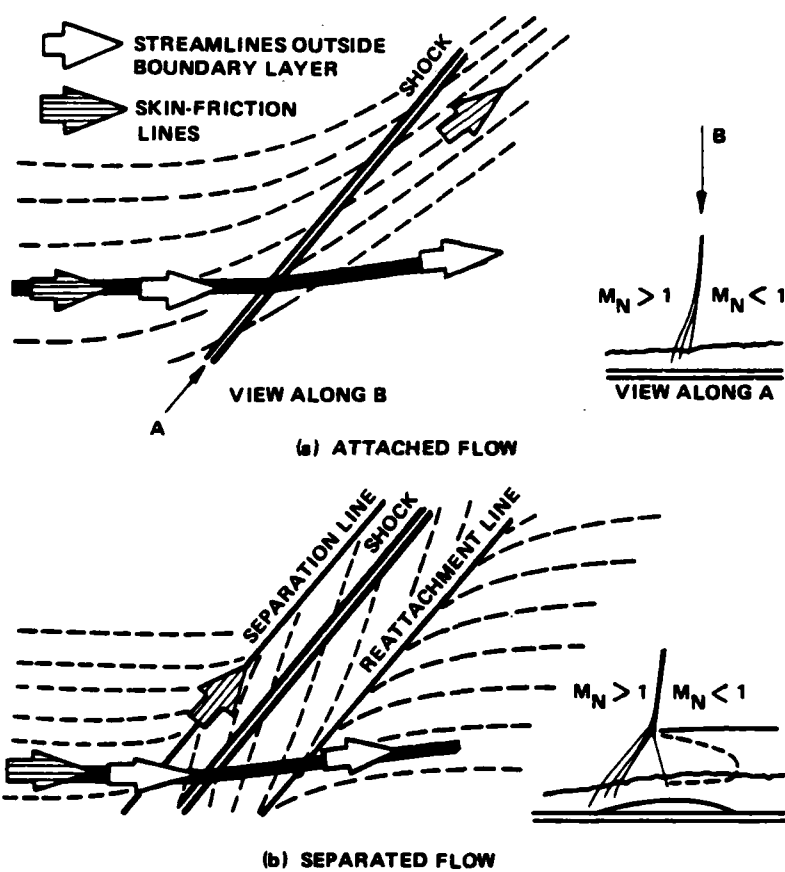
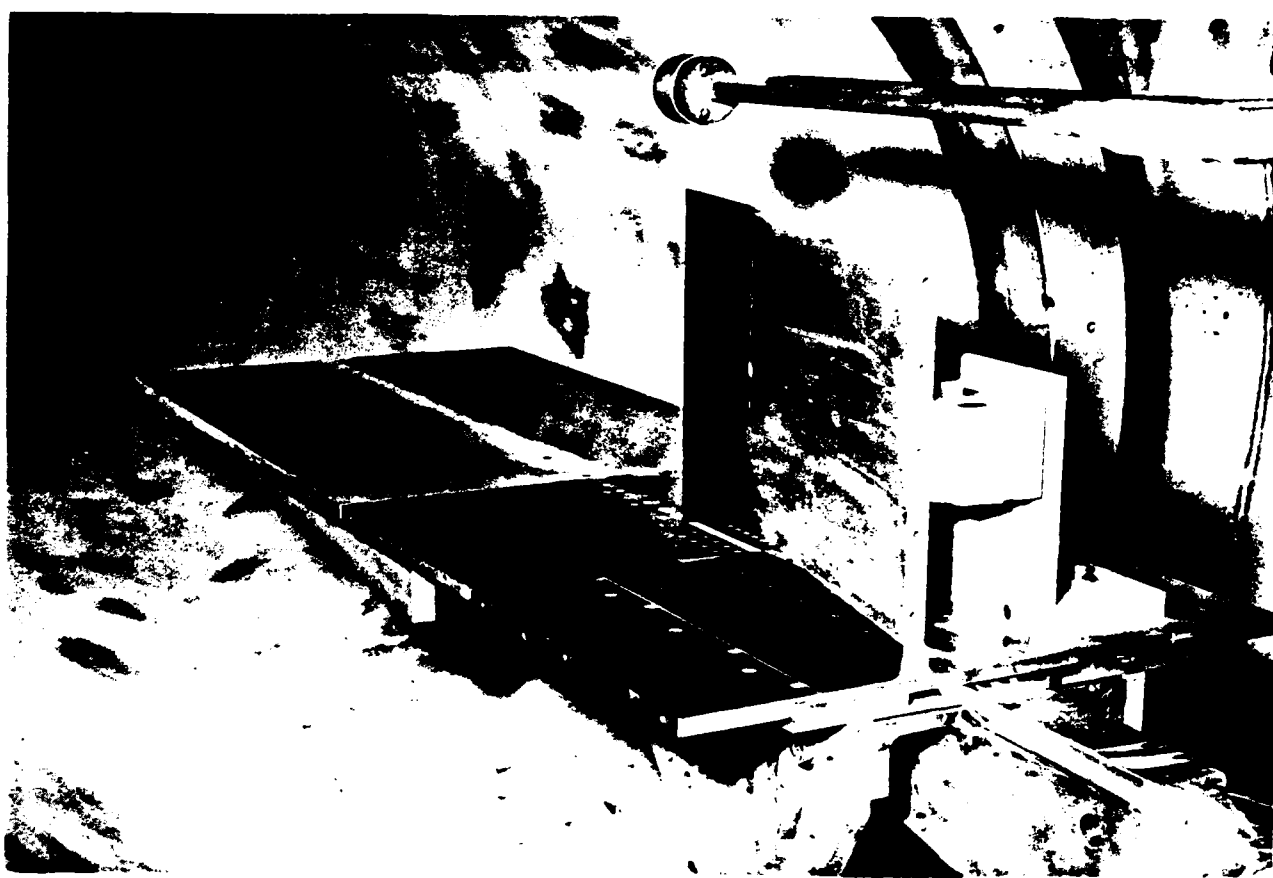


Figure 13 SCHEMATIC REPRESENTATION OF ATTACHED AND SEPARATED REGIONS IN SWEPT-SHOCK/BOUNDARY LAYER INTERACTIONS (REF. 34)

examination of surface oil streaks in the neighborhood of flow separation, are less sensitive methods for detecting flow separation than observations based on changes in the heat transfer distribution with increased interaction strength. In the current studies, we have used the incipient formation of a plateau in the heat transfer distribution, together with a marked increase in the fluctuation levels in the output of the thin film instrumentation, as marking the onset of flow separation.

Discussion of Results. The model used in the swept-shock/turbulent boundary layer study is shown in Figure 14. A 4-foot-long flat plate with a span of 2 feet was instrumented along three streamwise rays with heat transfer and pressure gages. We did not use skin friction gages in these studies because of the lengthy procedure which would be required to align the sensitive axis of the gage with local flow direction in the three-dimensional regions, and because we could use the thin film instrumentation to detect flow separation. The sharp fin was translated both normal and parallel to flow direction to place the major rays of instrumentation at different spanwise stations along the swept shock. Again, the high Mach numbers at which these studies were conducted mandated the use of large, highly stressed models.

The majority of experimental studies in this segment of the program were conducted at a Mach number of 11.2 and a Reynolds number, based on the distance to the beginning of the interaction, of  $50 \times 10^6$ . For such conditions (a typical set of freestream parameters is listed in Table 1), the boundary layer is fully turbulent ( $Re\delta = 2 \times 10^6$ ) upstream of the interaction. Measurements of the distributions of heat transfer and pressure were obtained on a series of ray's along the line of shock impingement for shock generator angles from 4 to 12.5 degrees. Here, we will discuss only the distributions obtained far from the tip of the fin, where the length of interaction ahead of the incident shock is invariant with distance along the shock (i.e., the cylindrical regime). Typical distributions of heat transfer and pressure along streamwise rays are shown in Figures 15 to 21 for shock generator angles of 5, 6.5, 7.5, 10 and 12.5 degrees. The heat transfer and pressure distributions for the interactions with the larger overall pressure rise ( $\alpha \approx 7.5^\circ$ ) exhibit well-defined plateau regions followed by a recompression rise to a region of relatively constant heat transfer and pressure adjacent to the fin. We observe the incipient formation of the plateau region and the accompanying increase in the fluctuation level exhibited in the output of the thin film gages at a fin angle of  $6.5^\circ$ . Thus, as shown in Figure 22, our measurements indicate that in hypersonic flow over highly-cooled walls, the turbulent boundary layer is more tenacious in resisting



**Figure 14 CORNER-INTERACTION MODEL**

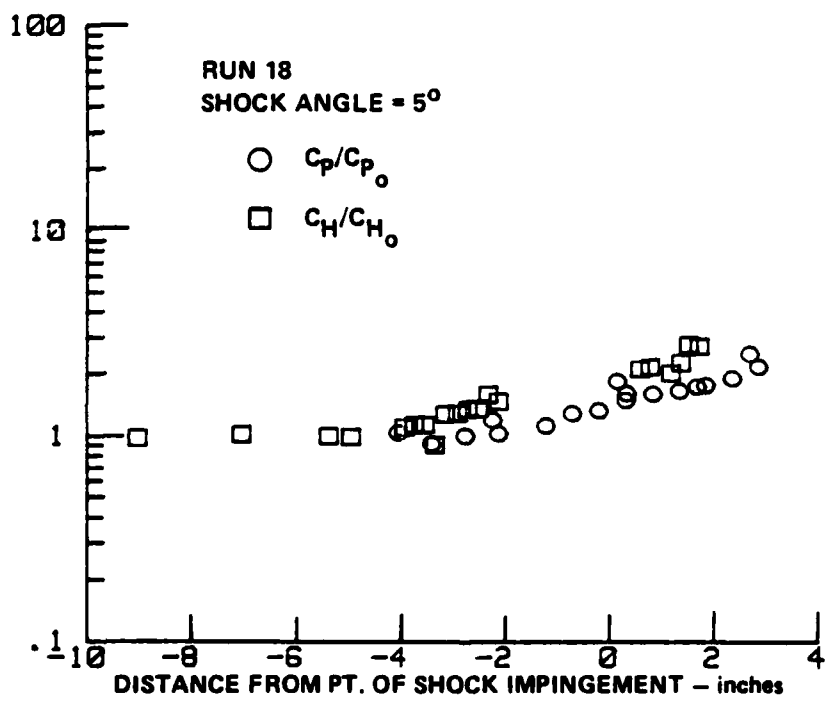


Figure 15 STREAMWISE DISTRIBUTION OF HEAT TRANSFER AND PRESSURE  
THROUGH SWEPT-SHOCK INTERACTION ( $\alpha = 5^\circ$ )

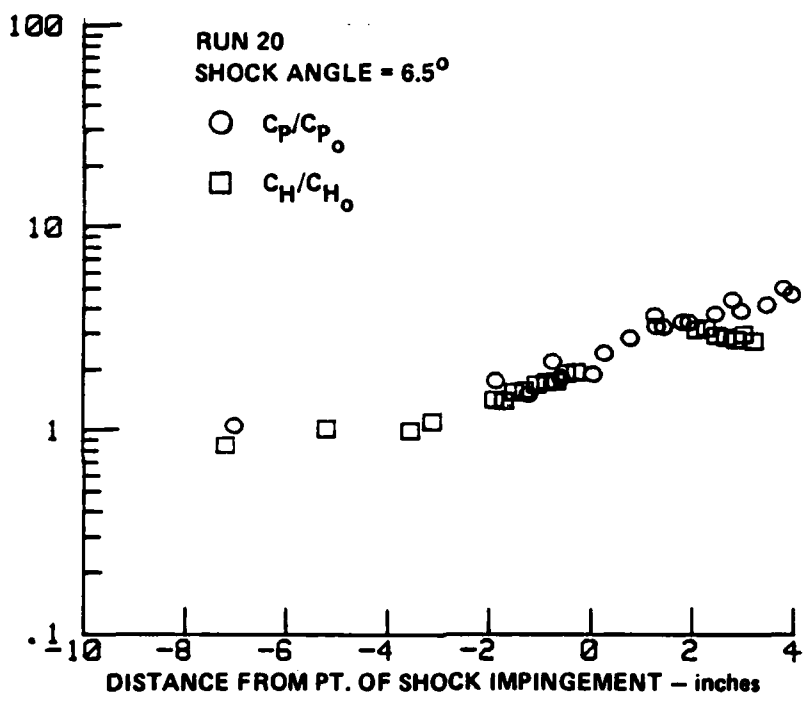


Figure 16 STREAMWISE DISTRIBUTION OF HEAT TRANSFER AND PRESSURE  
THROUGH SWEPT-SHOCK INTERACTION ( $\alpha = 6.5^{\circ}$ )

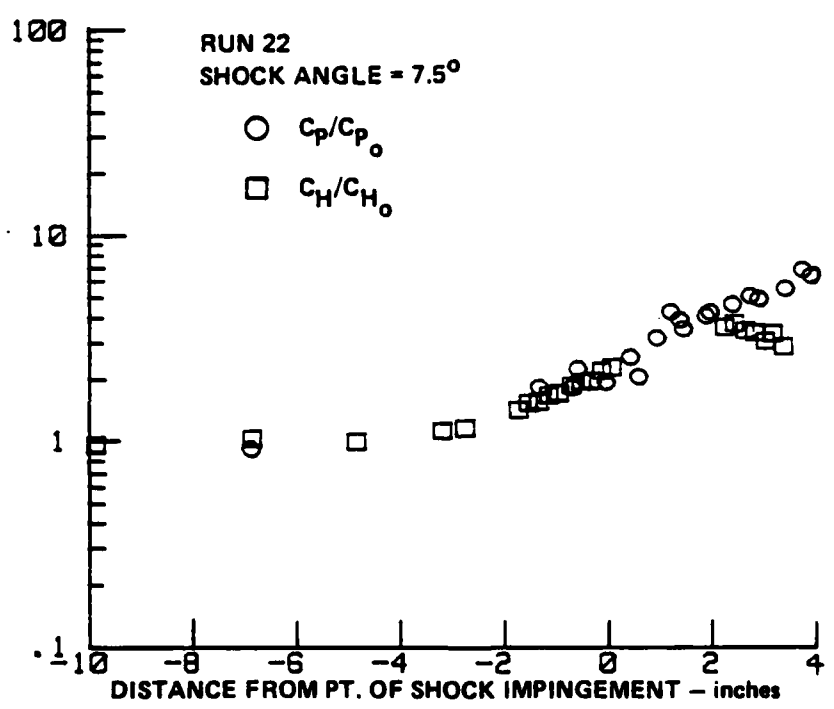


Figure 17 STREAMWISE DISTRIBUTION OF HEAT TRANSFER AND PRESSURE  
THROUGH SWEPT-SHOCK INTERACTION ( $\alpha = 7.5^\circ$ )

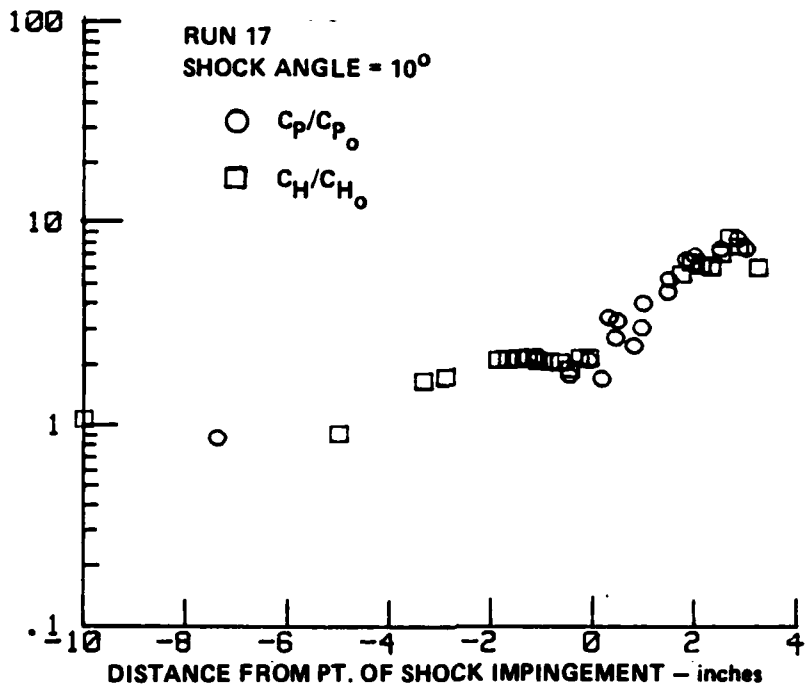


Figure 18 STREAMWISE DISTRIBUTION OF HEAT TRANSFER AND PRESSURE THROUGH SWEPT-SHOCK INTERACTION ( $\alpha = 10^{\circ}$ )

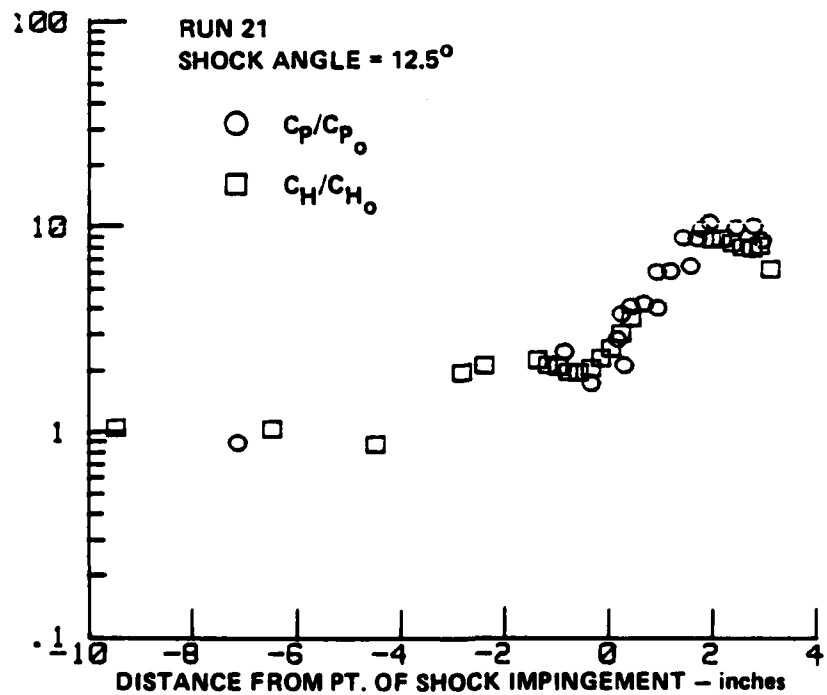
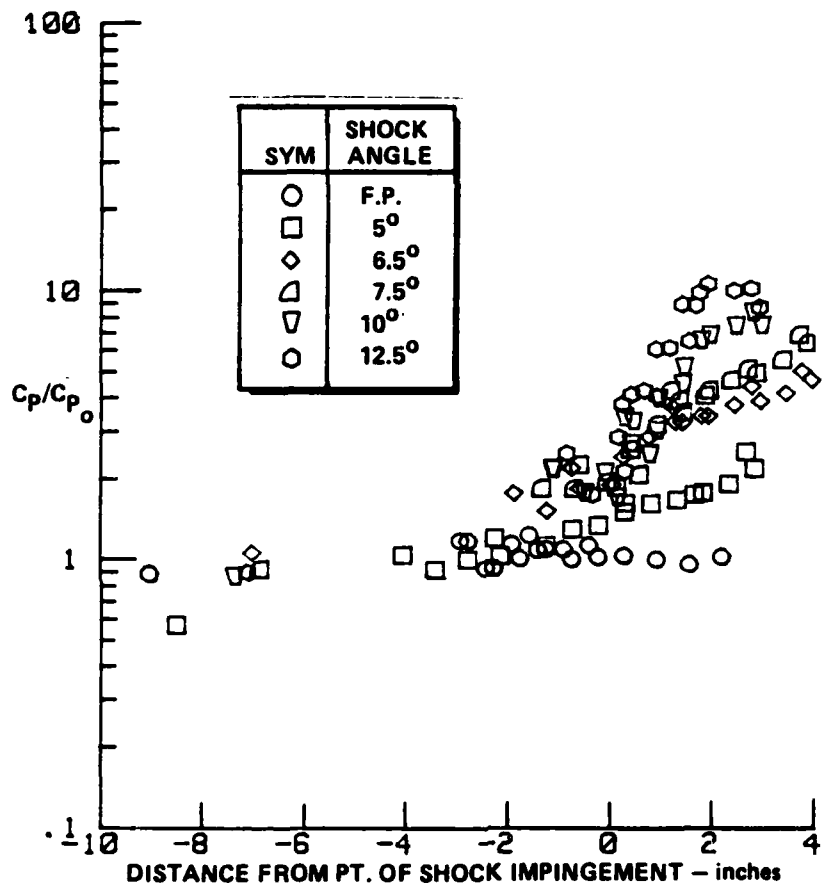
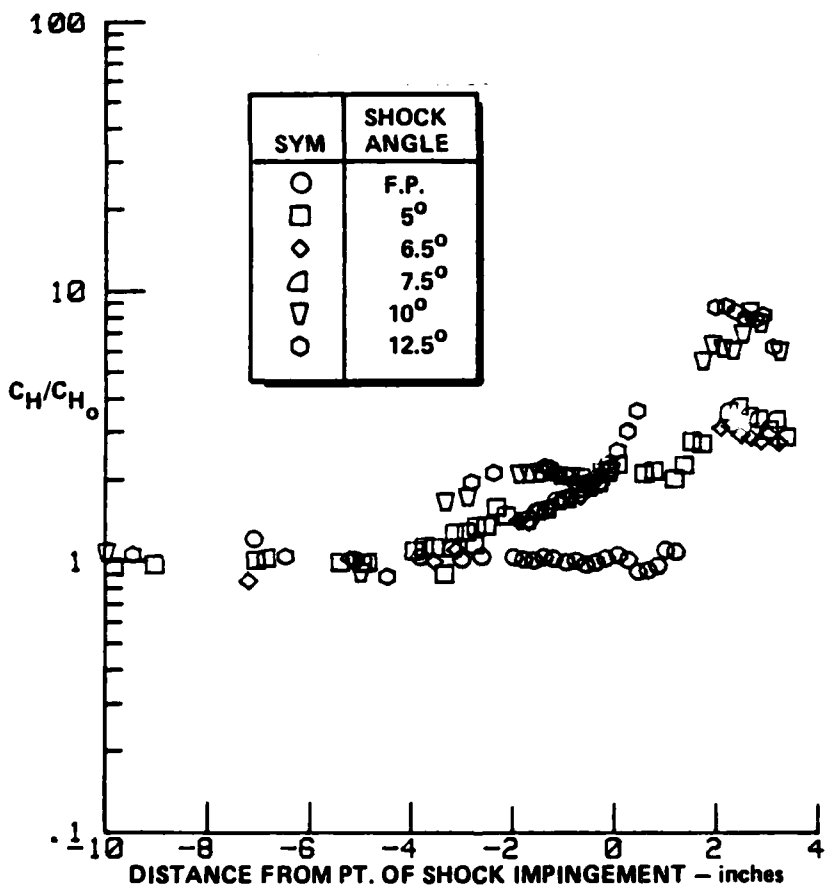


Figure 19 STREAMWISE DISTRIBUTION OF HEAT TRANSFER AND PRESSURE THROUGH SWEPT-SHOCK INTERACTION ( $\alpha = 12.5^{\circ}$ )



**Figure 20 VARIATION OF PRESSURE DISTRIBUTION THROUGH SWEPT-SHOCK INTERACTION REGIONS WITH SHOCK GENERATOR ANGLE**



**Figure 21 VARIATION OF HEAT TRANSFER DISTRIBUTION THROUGH SWEPT-SHOCK INTERACTION REGIONS WITH SHOCK GENERATOR ANGLE**

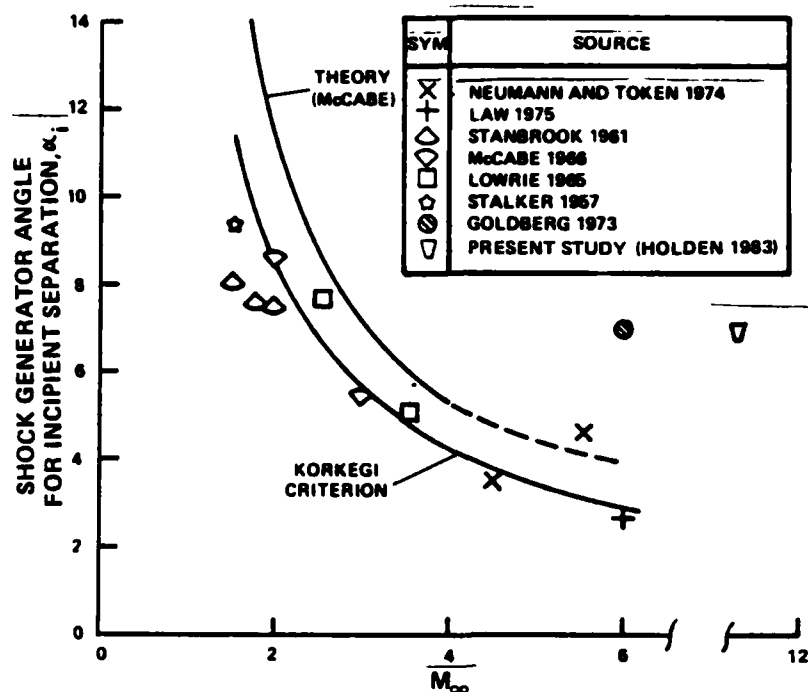


**Figure 22 VARIATION OF SHOCK GENERATOR ANGLE TO INDUCE INCIPIENT SEPARATION WITH MACH NUMBER**

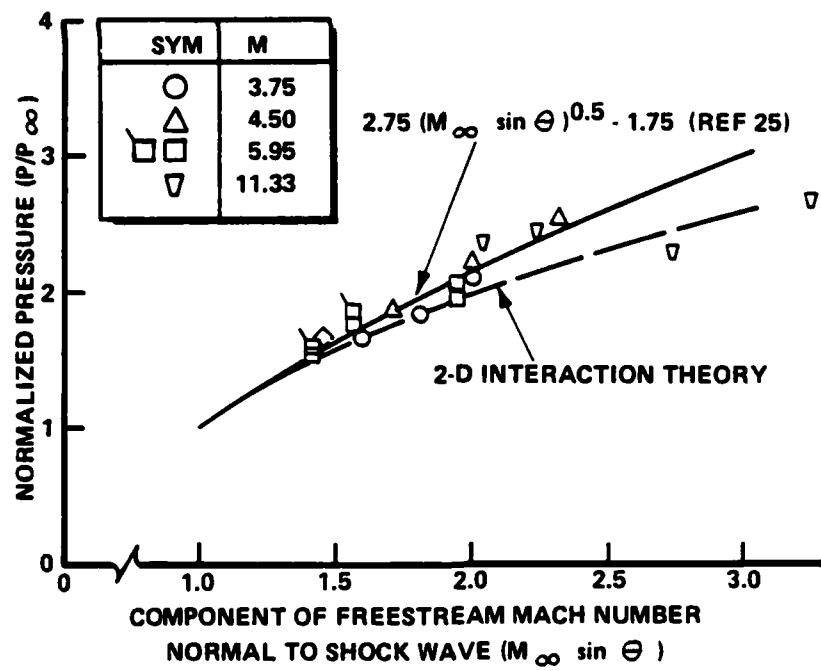


**Figure 23 CORRELATION OF PLATEAU PRESSURE MEASUREMENT FROM SWEPT-SHOCK INTERACTION STUDIES**

boundary layer separation than predicted by the methods derived by McCabe<sup>13</sup> and Korkegi<sup>21</sup>. Our measurements of the peak pressure ratio through the interaction and the plateau pressure rise are in better agreement with calculations based on an inviscid flow model in the 2D theory of Reshotko and Tucker<sup>33</sup> than the correlations of Scudari<sup>25</sup> as shown in Figure 23. However, we find that the ray on which peak heating is located is in reasonable agreement with the studies at lower Mach numbers by Token, as shown in Figure 24. As in our earlier studies of two-dimensional separated interaction regions (Figure 25), the peak heating can be related to the overall pressure rise by a simple power law relationship as shown in Figure 26. Figure 27 shows that the maximum pressure rise through the interaction region can be calculated with good accuracy from inviscid flow relationships. While there appears to be merit for the development of simple prediction methods in describing the flow in terms of the normal flow Mach number, this is clearly a gross oversimplification and it should be noted that the plateau pressure measurements obtained in the current study were relatively independent of  $M_\infty \sin \theta$ .

#### Studies of Shock Wave-Turbulent/Boundary Layer Interaction at a Cone/Flare Junction

In this segment of the study we set out to examine the characteristics of fully turbulent attached and separated interaction regions over cone/flare configurations in hypersonic high Reynolds number flows. In the initial phase of the study reported here the emphasis was on obtaining surface and flow visualisation measurements in preparation for a subsequent detailed probing of these flows. Finally we intended to obtain detailed flow field and surface heat transfer, skin friction and pressure measurements with which to perform comparisons with numerical solutions to the Navier-Stokes codes, with the object of investigating the modelling of turbulence in strong pressure gradients and separated flow at hypersonic speeds. One important objective of this current phase of the study was to determine the largest Mach number for which a fully turbulent corner interaction region could be developed over the cone/flare model in our experimental facilities because of our interest in obtaining measurements of direct relevance to the design and performance of maneuverable re-entry vehicles.

A major problem in performing detailed flow field surveys of turbulent boundary layers and regions of shock wave/turbulent boundary layer interaction in high Reynolds number hypersonic flow is that the wall layer, which contains the principal

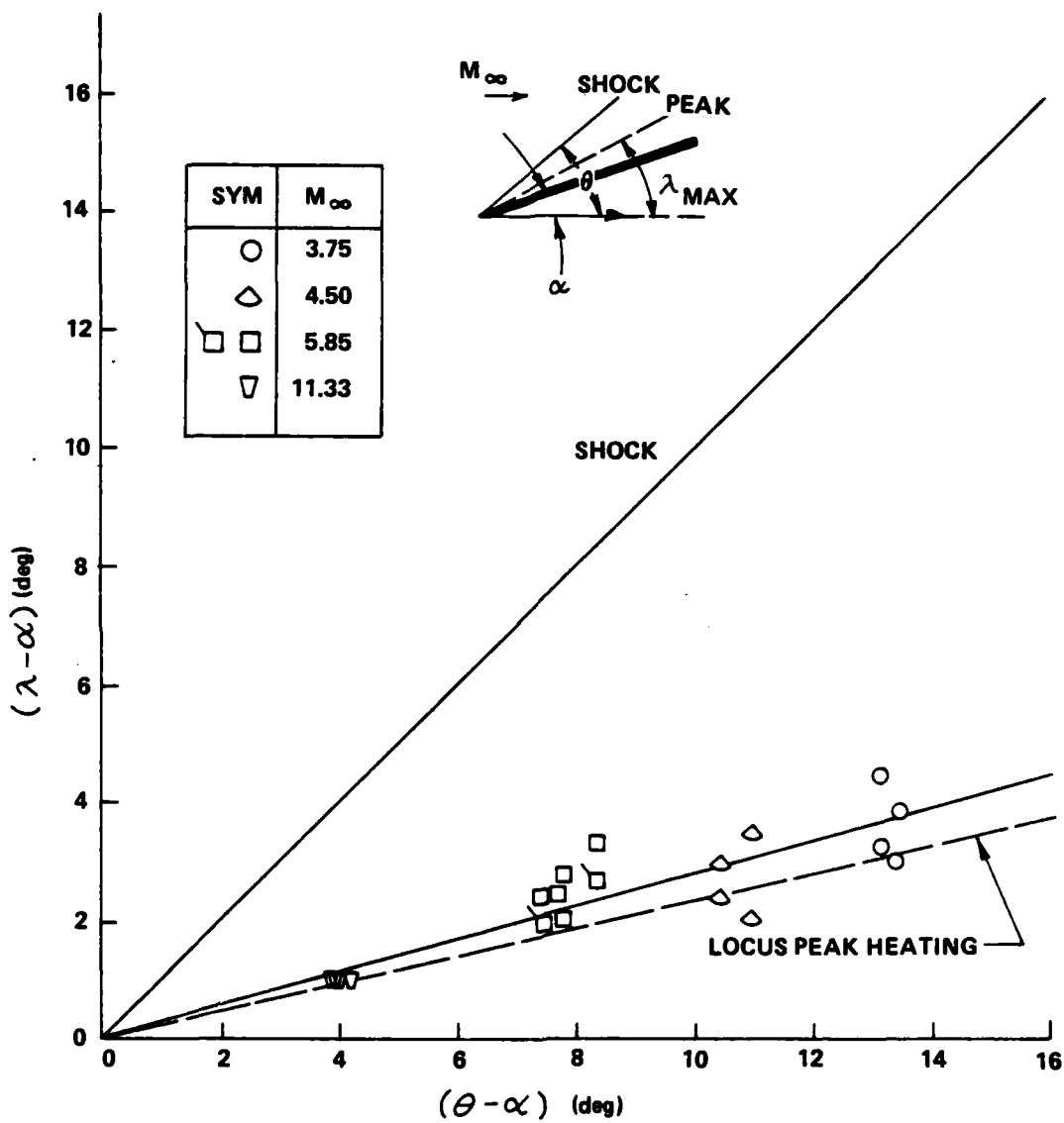


Figure 24 LOCATION OF BEGINNING OF PEAK HEATING REGION

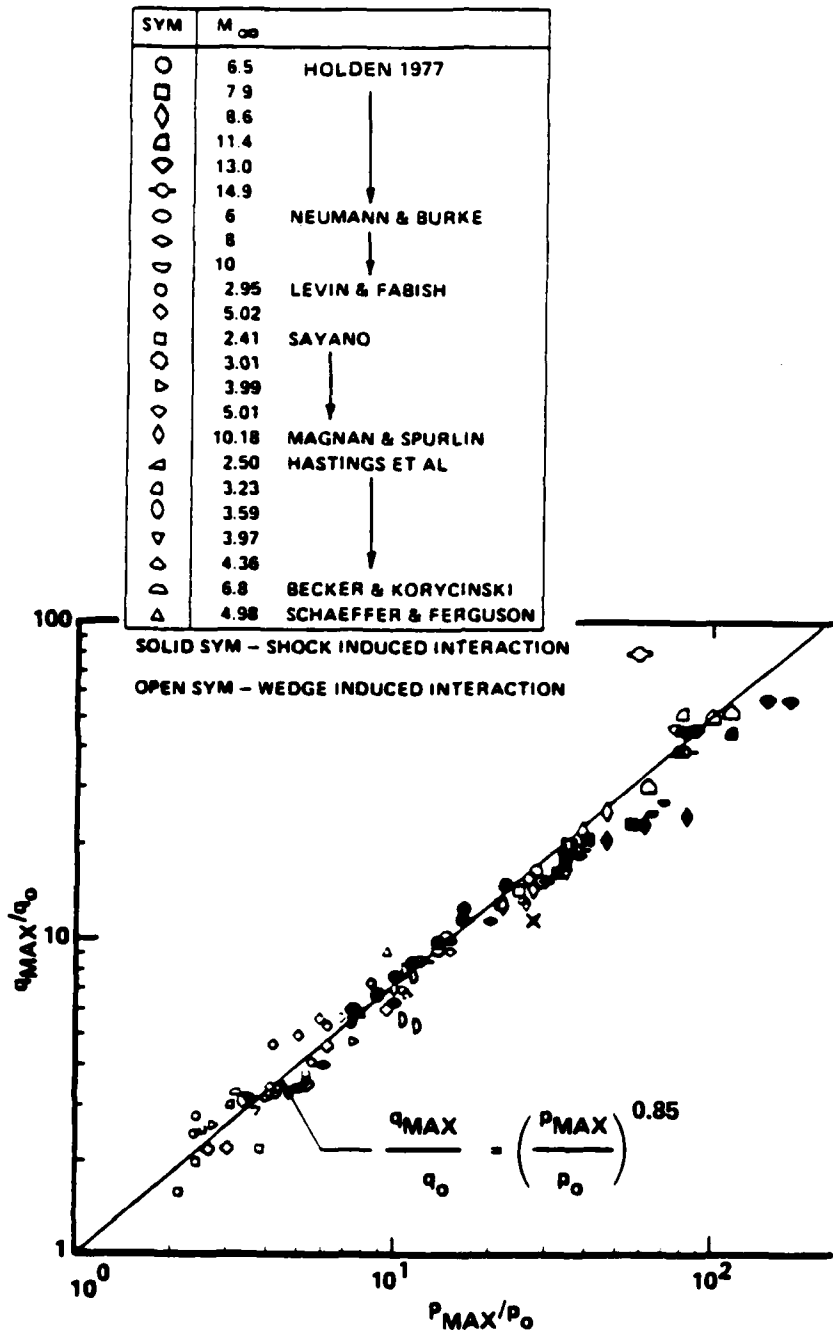


Figure 25 CORRELATION OF MAXIMUM HEATING RATE IN WEDGE- AND EXTERNALLY-GENERATED SHOCK-INDUCED TURBULENT SEPARATED FLOWS

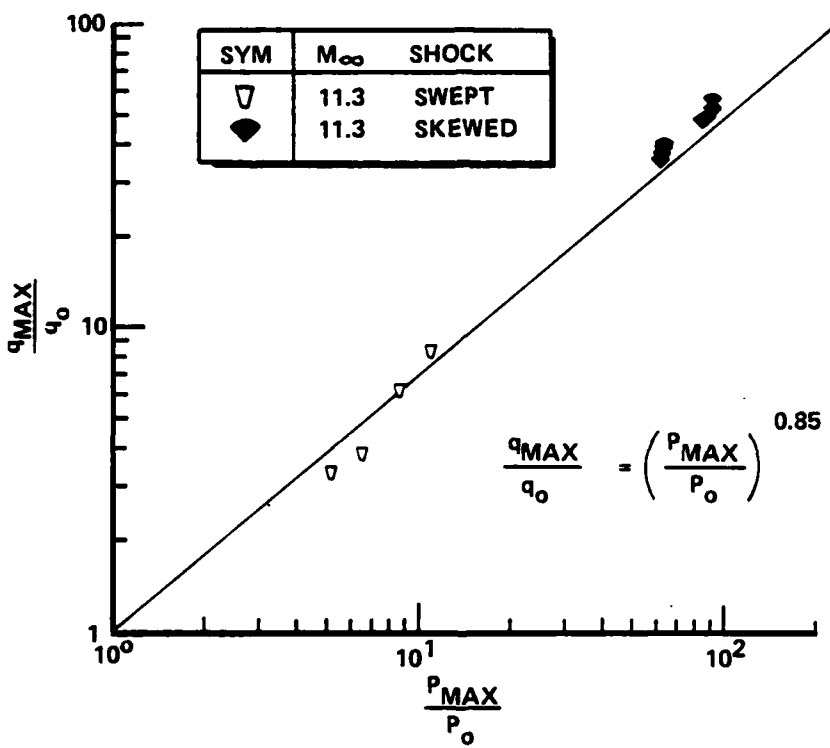


Figure 26 CORRELATION OF PEAK HEATING RATES IN SKEWED- AND SWEPT-SHOCK INTERACTION REGIONS

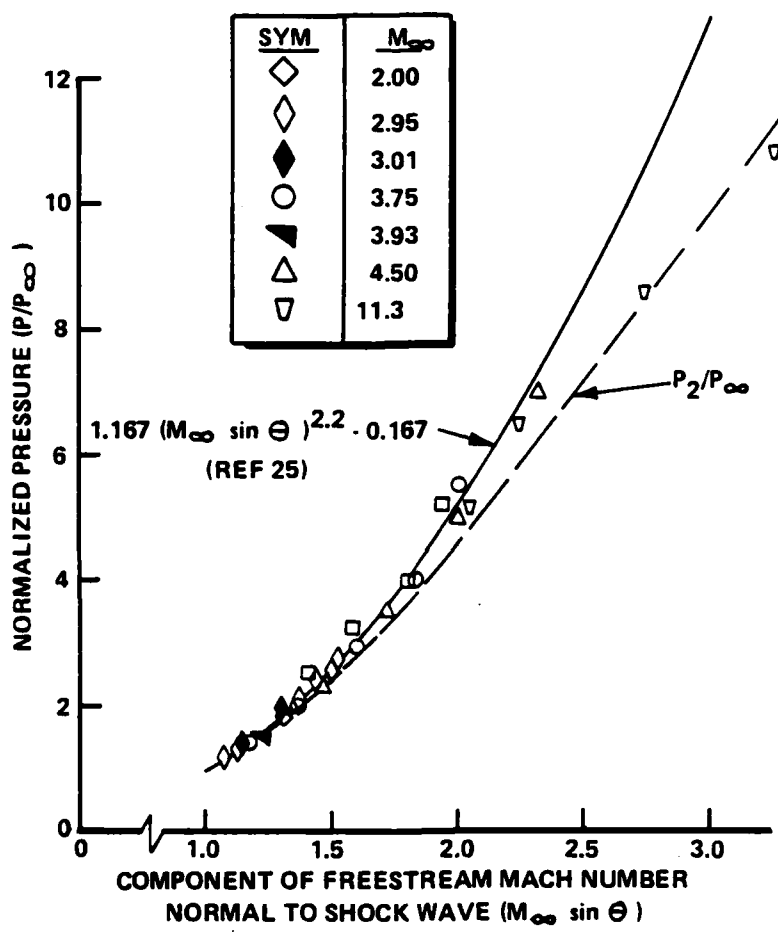


Figure 27 CORRELATION OF MAXIMUM PRESSURES RECORDED IN SWEPT-SHOCK INTERACTION REGIONS

information on the structure of the turbulent boundary layer and the mechanisms involved with boundary layer separation, is of the order of 10% of the boundary layer thickness. Thus practically large boundary layers (1 inch) are required to obtain a definitive number of data points from the wall layer. Because of the basic insensitivity of turbulent boundary layer growth to Reynolds number, it is necessary to use large models or perform tests on tunnel walls to obtain these thick boundary layers. Tests on tunnel walls are particularly unattractive in hypersonic flow because of significant turbulent non-equilibrium effects generated in the boundary layer by the strong nozzle expansion. While employing large flat plate models is the most effective way of generating thick boundary layers, experimental studies of separated two-dimensional interaction regions on models of finite span with thick boundary layers nearly always fall victim to ill-defined boundary conditions. We therefore elected to perform our studies using a large slender cone/flare model. A cone angle of  $6^{\circ}$  was selected to provide local Mach numbers and Reynolds numbers typical of those on maneuvering re-entry vehicles. The cone length (11 ft.), and the positioning within the tunnel was selected on the basis of simple calculations of the maximum length of cone over which uniform flow could be established within the further constraints of tunnel blockage and the loading of the model support. Therefore, an important objective of this initial study was to establish whether these calculations were correct. A schematic diagram of the sharp cone model shown installed in the 96 Inch Shock Tunnel is shown in Figure 28. Earlier we have obtained pressure and heat transfer measurements on this model capped with a spherical nosetip as shown in Figure 29. A comparison between the pressure measurements made on this model, on a much smaller model of identical shape, and calculations based on the NSWC blunted cone code is shown in Figure 30. It can be seen that the pressure measurements on the large slender cone, which are a sensitive indicator of flow quality, are in excellent agreement with both theory and earlier measurements.

The studies of the flow over the sharp cone model and the turbulent interaction regions on the cone/flare configurations were conducted in the Calspan 96-Inch Shock Tunnel at Mach numbers of 11, 13 and 16 for Reynolds numbers from  $30 \times 10^6$  to  $80 \times 10^6$ . The nominal test conditions at which the studies were conducted are listed in Table 2. The large cone/flare model, which is shown installed in the test section of the 96-Inch Tunnel in Figure 31, was fitted with flares with angles of 30 and 36 degrees relative to the surface of the basic cone. Distributions of heat transfer and pressure as well as schlierer photographs were obtained for each model configuration

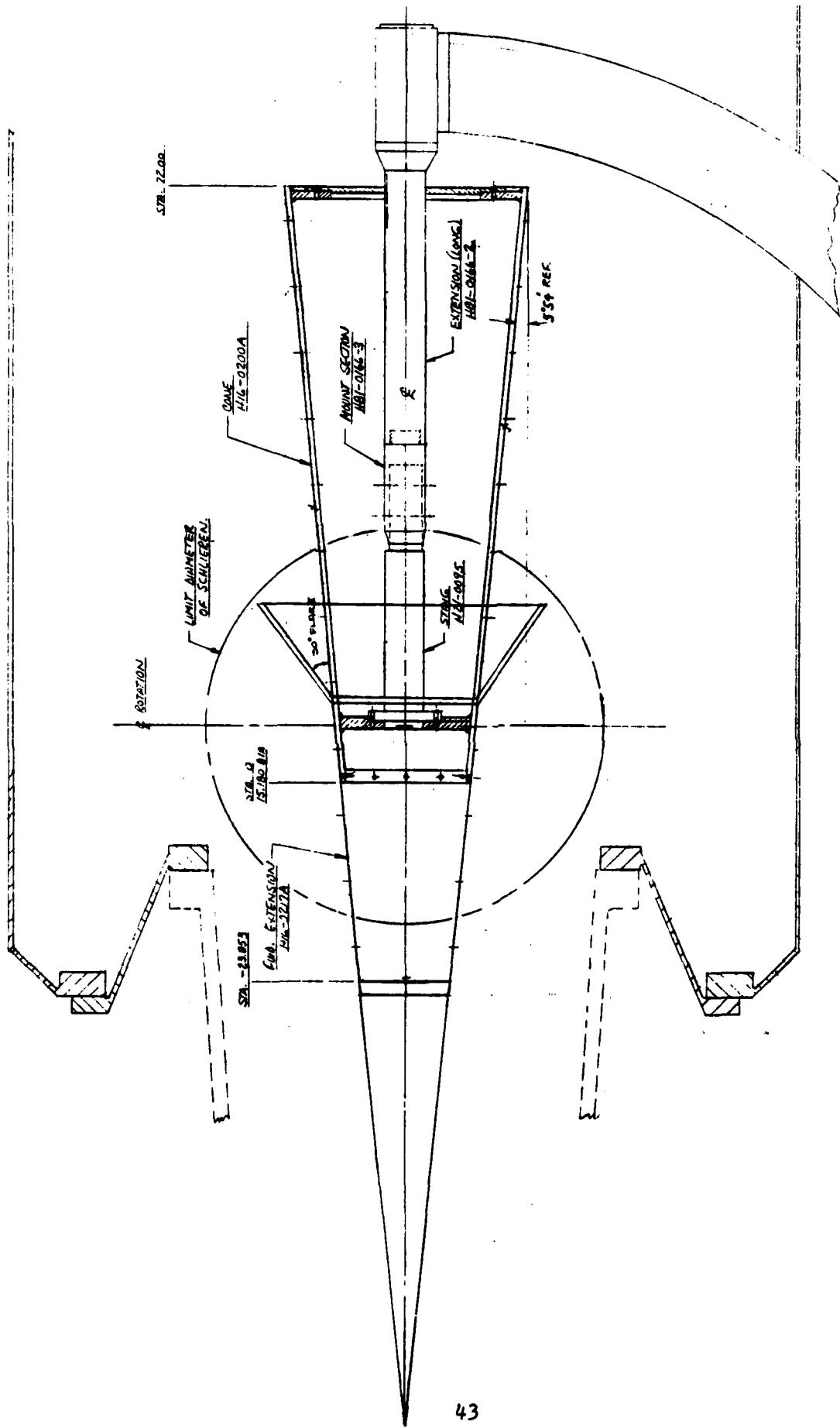


Figure 28 SCHEMATIC DIAGRAM OF LARGE 6° CONE WITH FLARE USED IN STUDIES

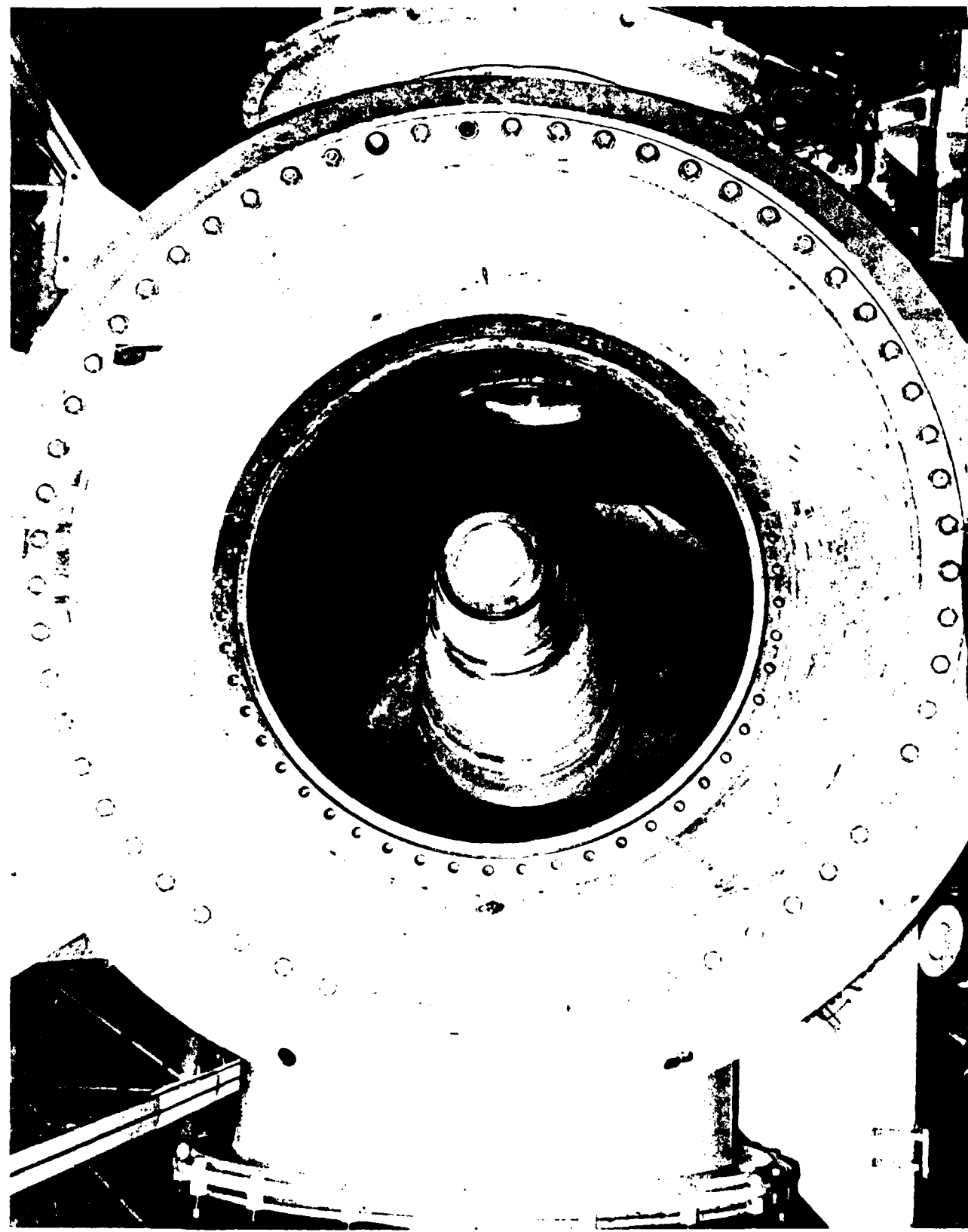


Figure 29 SPHERICAL NOSETIP MOUNTED ON LARGE 6° CONE

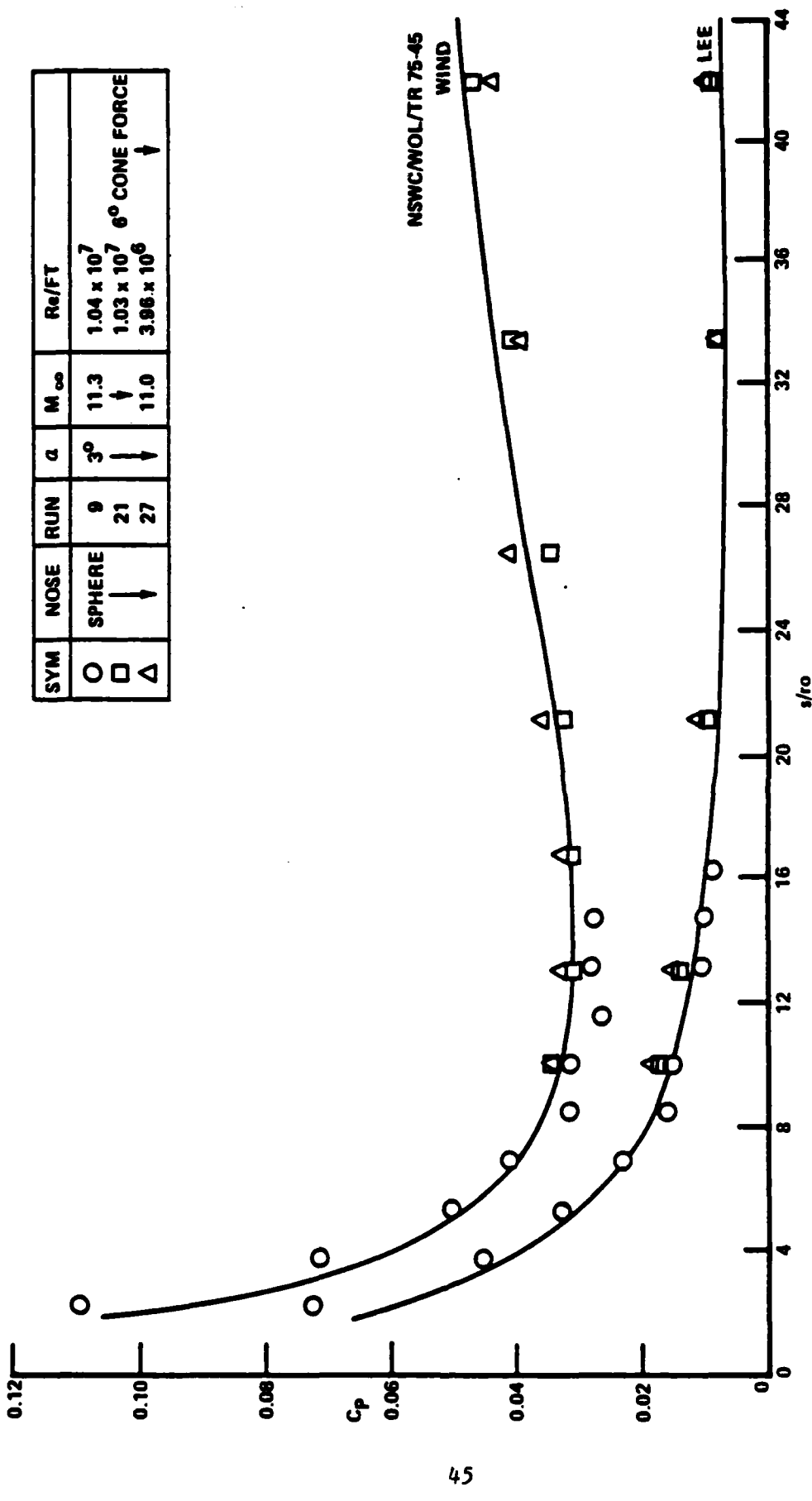


Figure 30 COMPARISON BETWEEN MEASURED PRESSURE DISTRIBUTION AND THEORY FOR SPHERICALLY CAPPED 6° CONE AT 3° INCIDENCE

**Table 2**  
**TEST CONDITIONS FOR THE CONE/FLARE STUDY**

M <sub>i</sub>	3.345E+00	3.633E+00	4.200E+00
P <sub>o</sub> PSIA	7.216E+03	1.760E+04	1.705E+04
H <sub>o</sub>	1.825E+07	2.147E+07	2.795E+07
T <sub>o</sub> °R	2.717E+03	3.104E+03	3.875E+03
M	1.096E+03	1.301E+01	1.543E+01
U FT/SEC	5.922E+03	6.458E+03	7.404E+03
T °R	1.214E+02	1.026E+02	9.574E+01
P PSIA	9.172E-02	7.345E-02	1.860E-02
Q PSIA	7.721E+00	8.712E+00	3.104E+00
RHO	6.340E-05	6.038E-05	1.631E-05
Mu	1.021E-07	8.634E-08	8.054E-08
RE/FT	3.680E+06	4.544E+06	1.499E+06
PITOT PSIA	1.431E+01	1.619E+01	5.798E+00



Figure 31 SHARP 6° CONE/30° FLARE MODEL INSTALLED IN CALSPAN'S 96" SHOCK TUNNEL

and test condition. The distributions of heat transfer and pressure in attached and separated flow over the cone/flare model with flare angles of 30 and 36 degrees respectively, are shown in Figures 32, 34, 36 and 33, 35 respectively. Shown in Figures 32a to 35a are comparisons between the measured pressures and calculations based on simple inviscid flow theory. The good agreement between the pressure measurement on the cone and flare, and theory for both attached and separated interactions, in a regime where pressure measurements are very sensitive to flow uniformity, gives us a high degree of confidence in our selection of the model scale and positioning. For the flow over the  $36^\circ$  flare configuration it is clear from the well-defined plateau region in both the heat transfer and pressure distribution on the cone just upstream of the flare that a well-separated flow is induced. The schlieren photographs of the flows over this latter configuration, shown in Figures 33a and 35a, clearly indicate the presence of a separation shock followed by a straight shear layer bounding constant pressure separated region. In contrast, in the attached flow over the  $30^\circ$  flare the shock emanates almost directly from the cone-flare junction. The measurements of pressure and heat transfer on the flare for both model configurations exhibit two levels; the first, just downstream of the interaction, corresponds to a locally two-dimensional compression; further downstream, the pressure and heat transfer rates approach those for a conical surface. The pressure levels computed from inviscid flow considerations are shown for reference in Figures 32a and 33a. A similar set of measurements are shown for the Mach 13 test condition in Figures 34a and 35a. Again we observe a well separated flow over the model with the  $36^\circ$  flare, and it is of interest to note that the scale of interaction region at the higher Mach number does not differ significantly from that at Mach 11. The measurements incipient separation and the heat transfer and pressure in the plateau and peak heating regions are compared with those made in the earlier two-dimensional studies in Figures 37 to 40. The good agreement between these sets of data, which reflects in part the locally two-dimensional character of the interaction at the cone/flare junction, gives us additional confidence in our design of this experiment. Later we plan to compare the surface measurements with Navier-Stokes solutions; however, based on the success of these experiments, our next objective is to obtain detailed flow field measurements in both attached and separated flows over the configurations studied here.

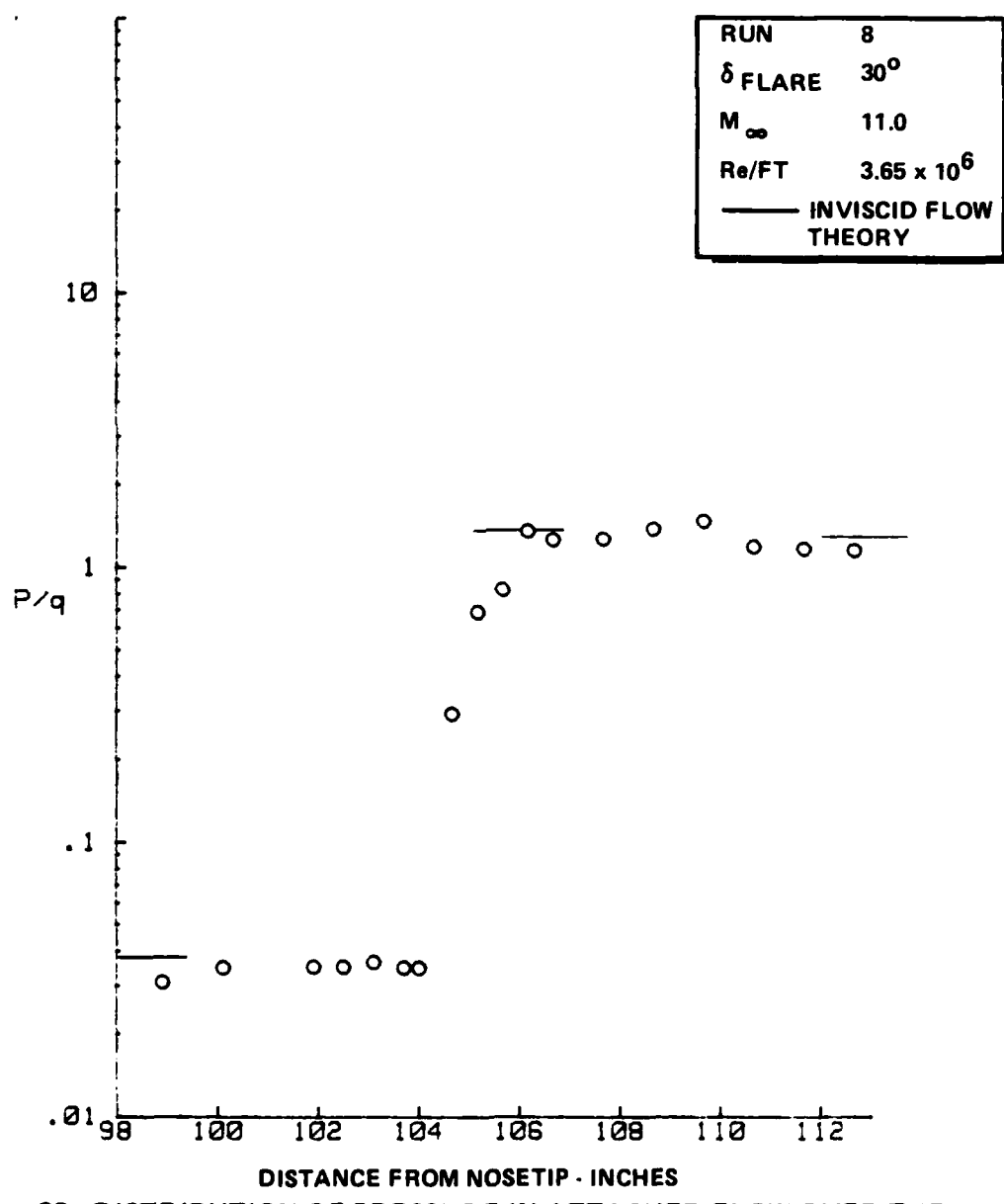
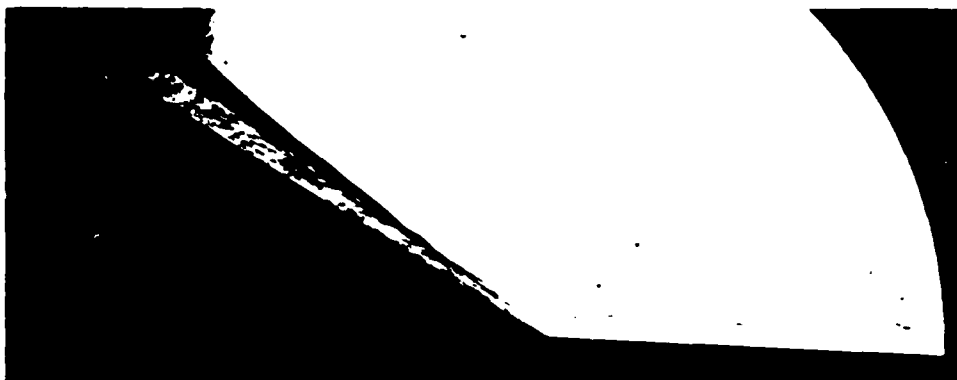


Figure 32a DISTRIBUTION OF PRESSURE IN ATTACHED FLOW OVER THE  
LARGE  $6^\circ$  CONE/ $30^\circ$  FLARE CONFIGURATION

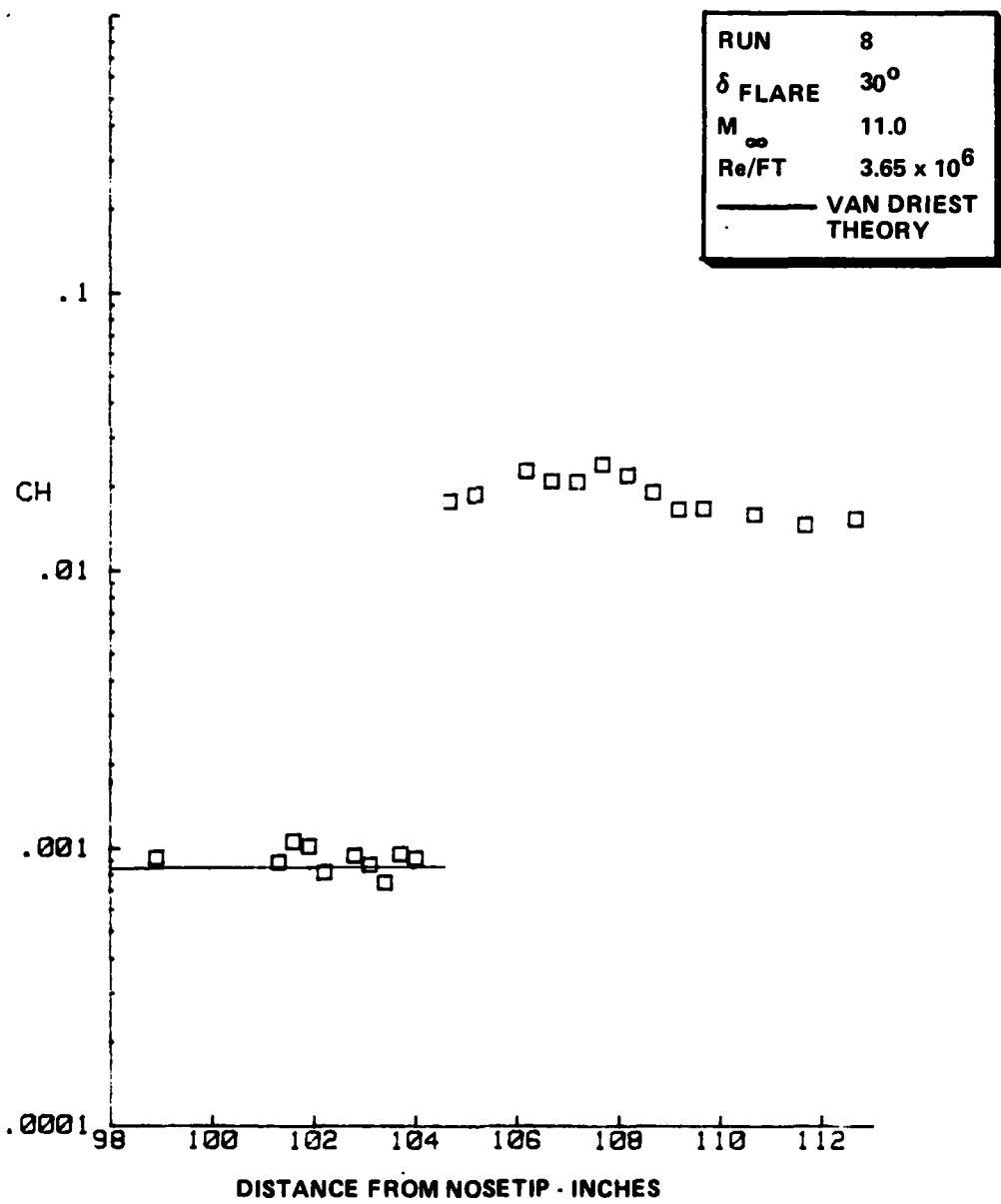


Figure 32b DISTRIBUTION OF HEAT TRANSFER IN ATTACHED FLOW OVER THE LARGE 6° CONE/30° FLARE CONFIGURATION

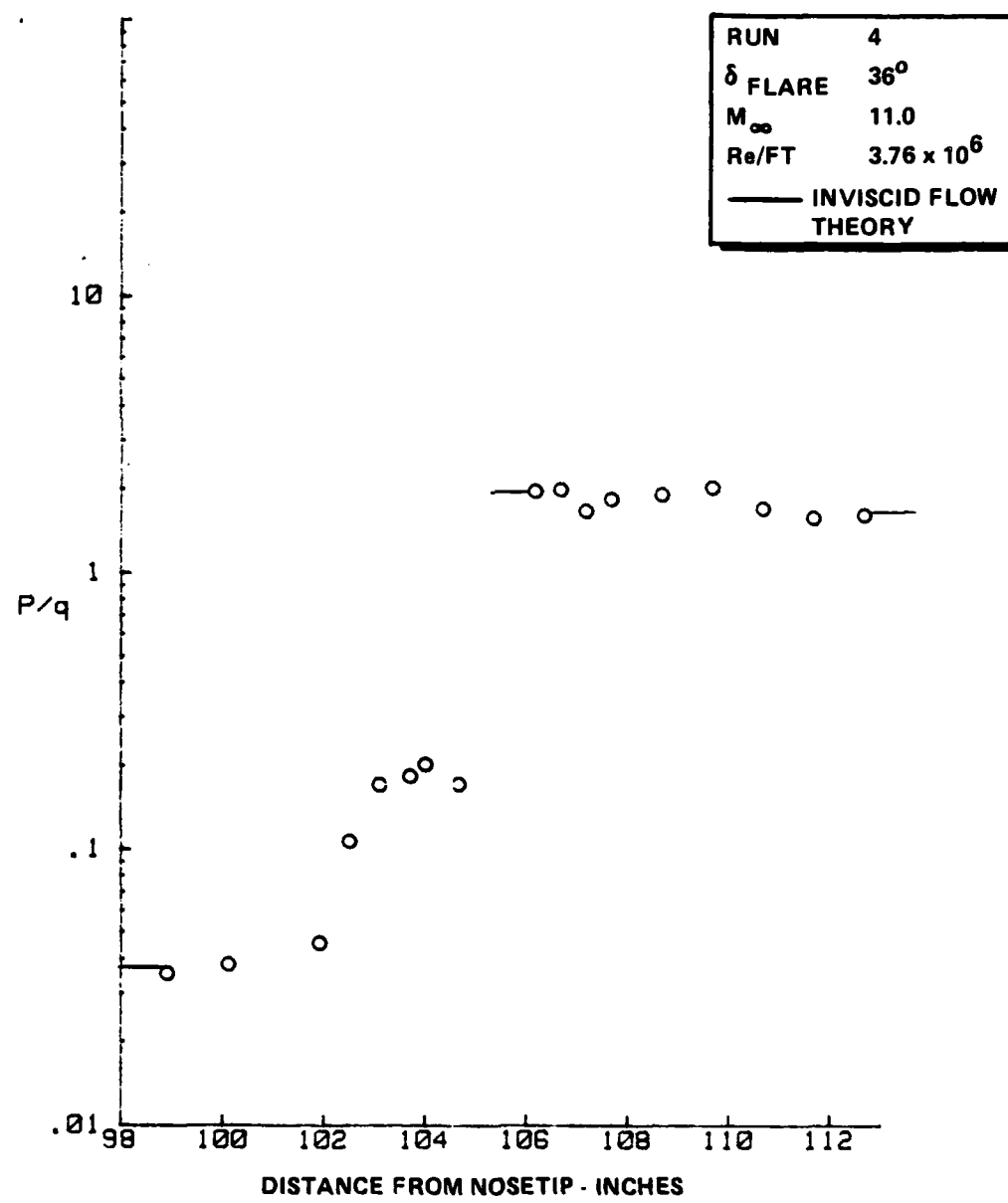
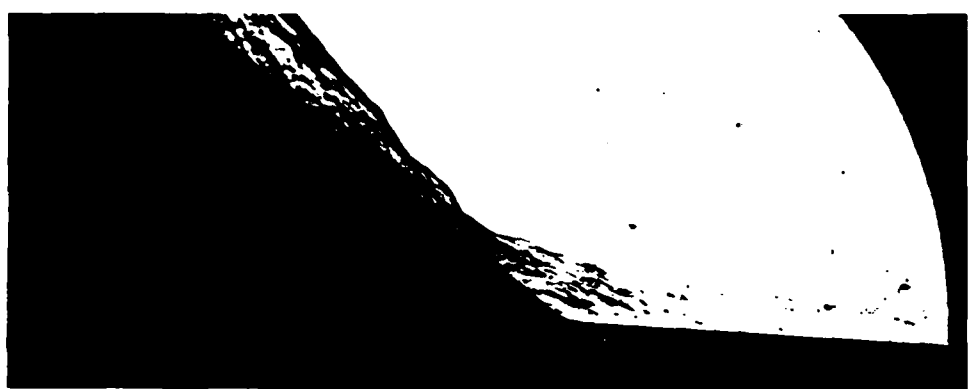


Figure 33a DISTRIBUTION OF PRESSURE IN SEPARATED FLOW OVER THE LARGE  $6^\circ$  CONE/ $36^\circ$  FLARE CONFIGURATION

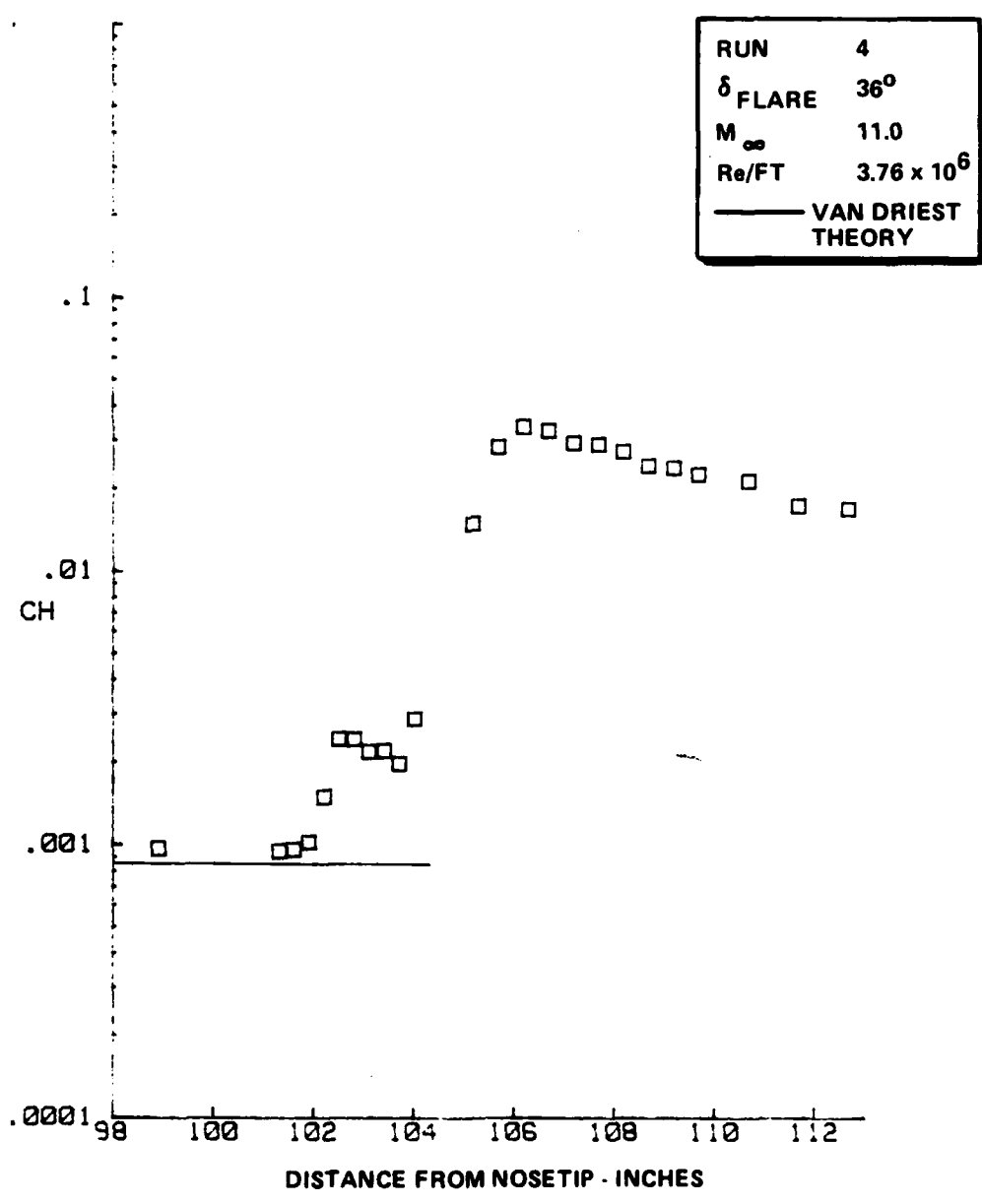


Figure 33b DISTRIBUTION OF HEAT TRANSFER IN SEPARATED FLOW OVER THE LARGE  $6^{\circ}$  CONE/ $36^{\circ}$  FLARE CONFIGURATION

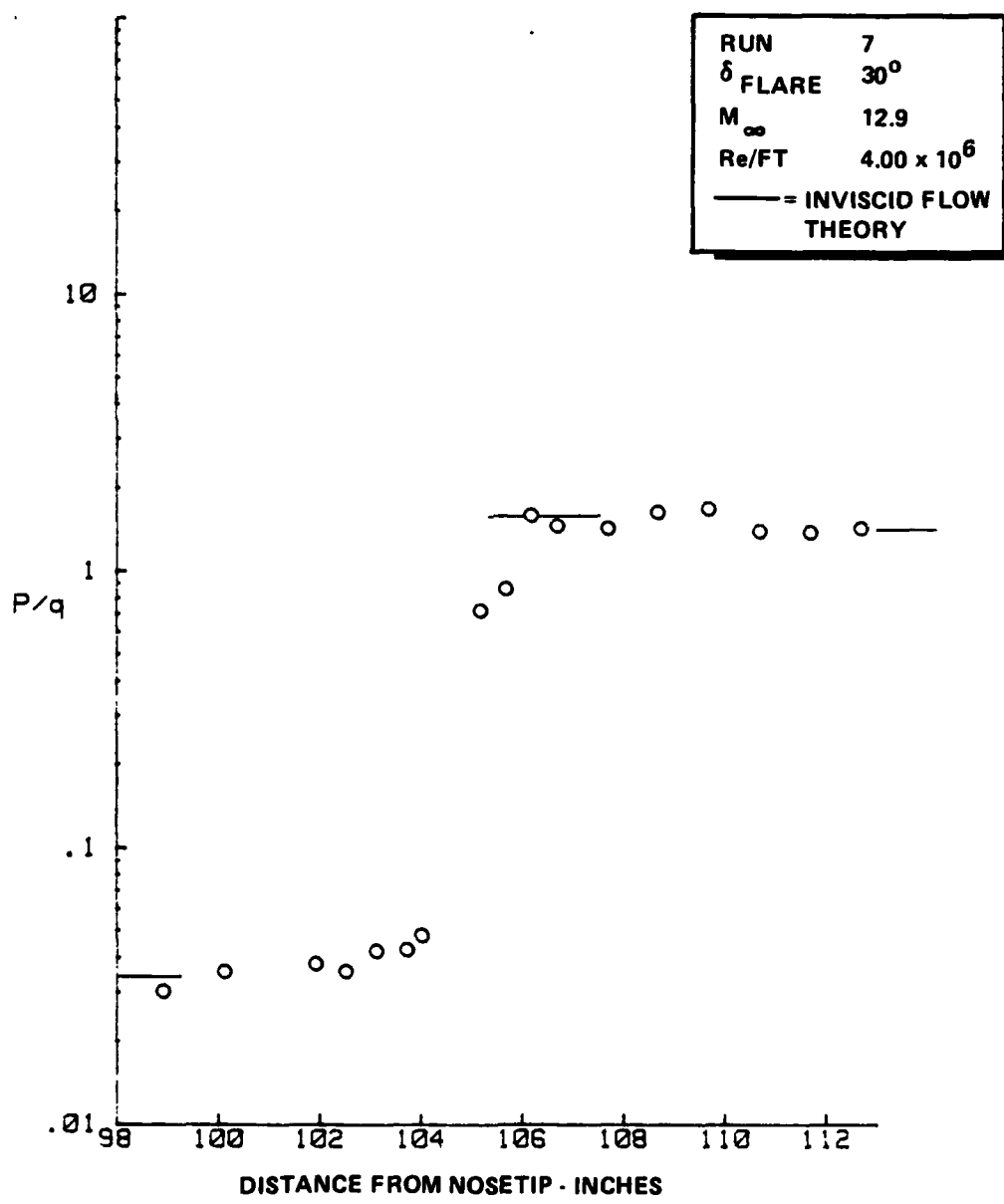
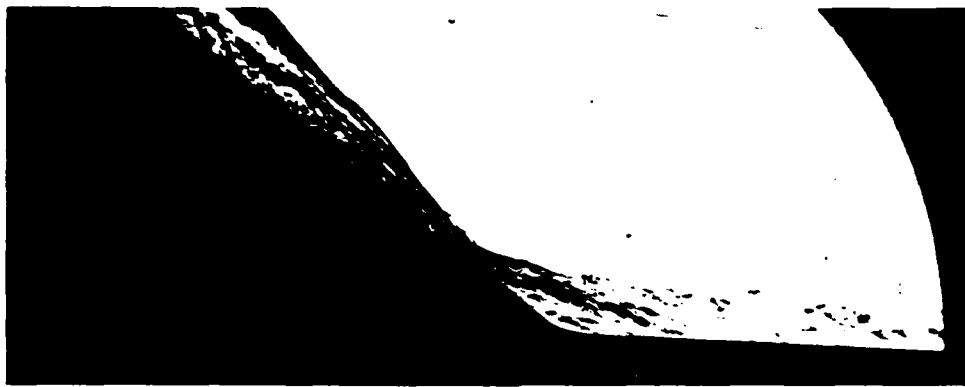


Figure 34a DISTRIBUTION OF PRESSURE IN ATTACHED FLOW OVER THE LARGE  $6^\circ$  CONE/ $30^\circ$  FLARE CONFIGURATION

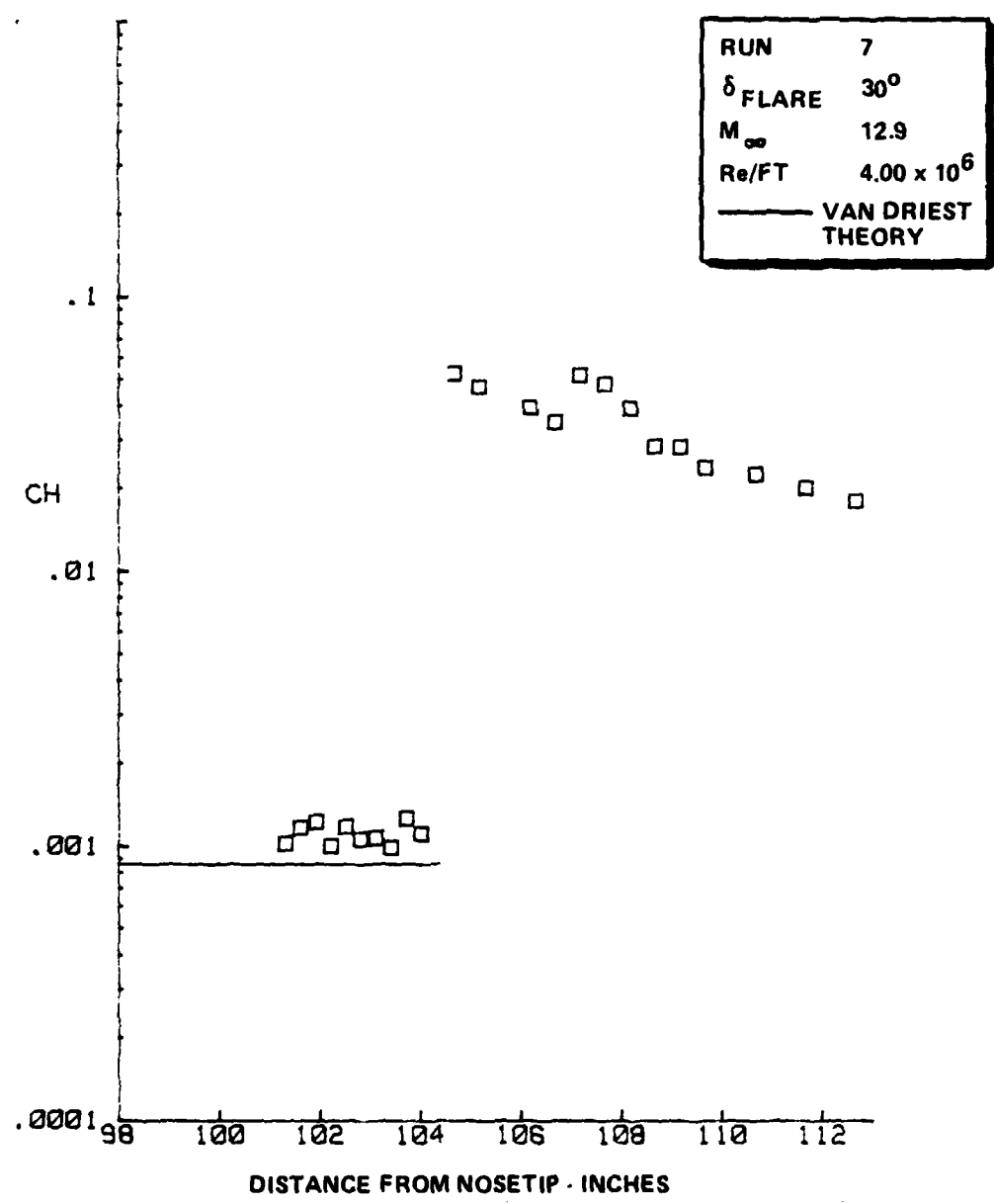


Figure 34b DISTRIBUTION OF HEAT TRANSFER IN ATTACHED FLOW OVER THE LARGE  $6^\circ$  CONE/ $30^\circ$  FLARE CONFIGURATION

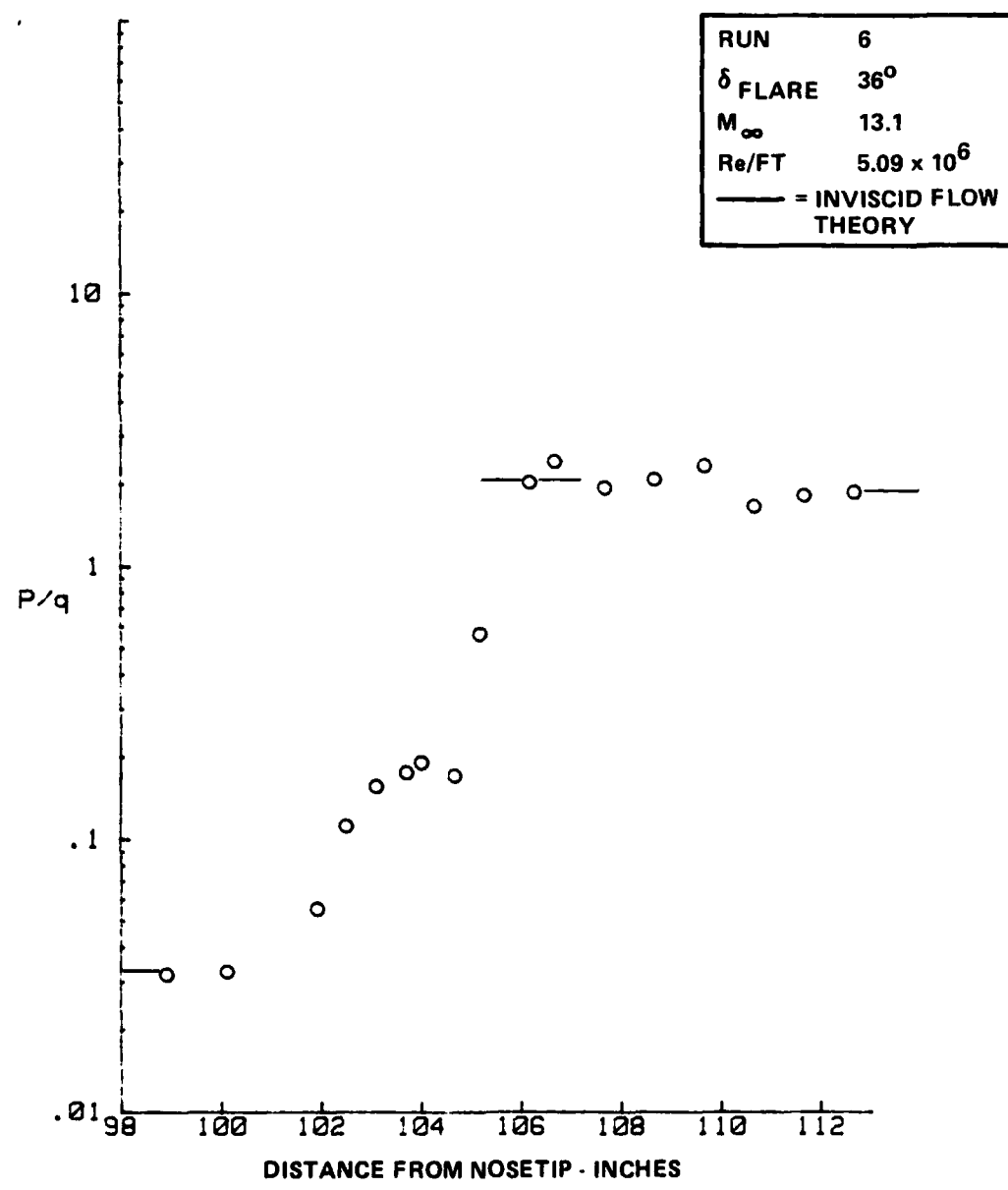


Figure 35a DISTRIBUTION OF PRESSURE IN SEPARATED FLOW OVER THE  
LARGE 6° CONE/36° FLARE CONFIGURATION

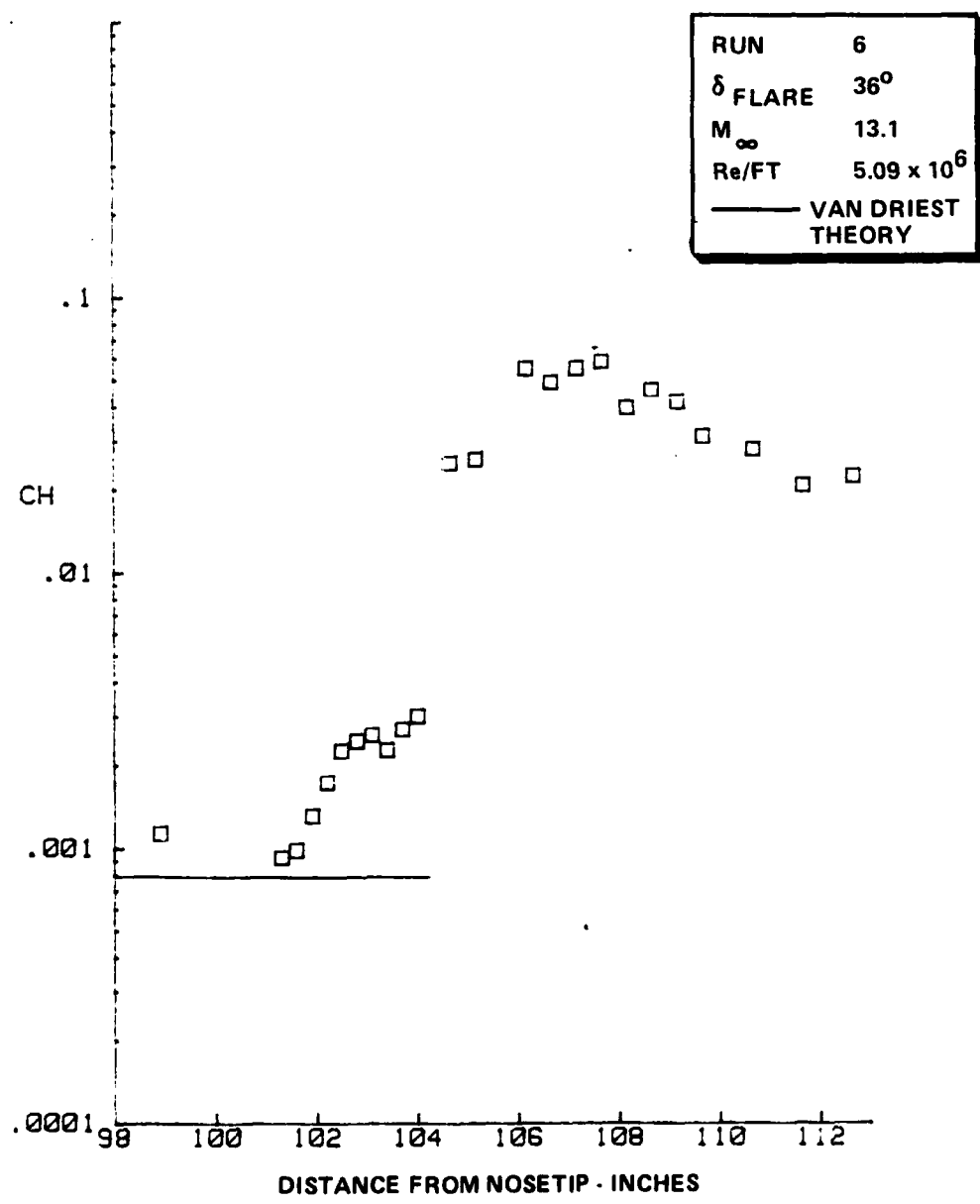


Figure 35b DISTRIBUTION OF HEAT TRANSFER IN SEPARATED FLOW OVER THE LARGE  $6^\circ$  CONE/ $36^\circ$  FLARE CONFIGURATION

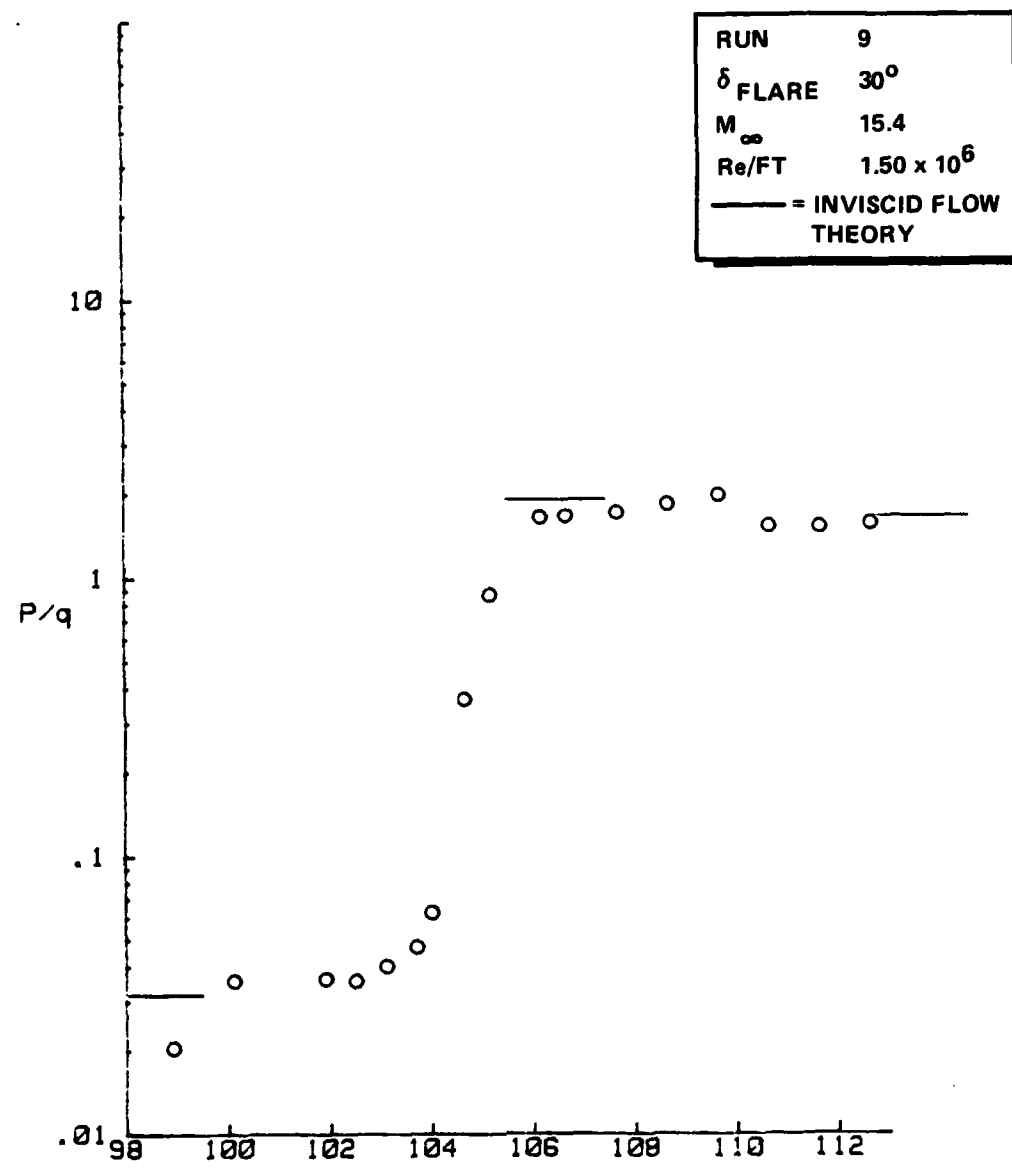
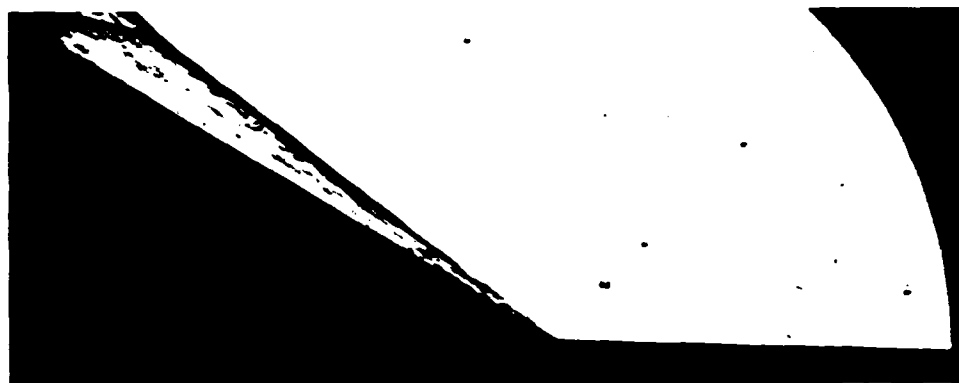


Figure 36a DISTRIBUTION OF PRESSURE IN ATTACHED FLOW OVER THE LARGE 6° CONE/30° FLARE CONFIGURATION

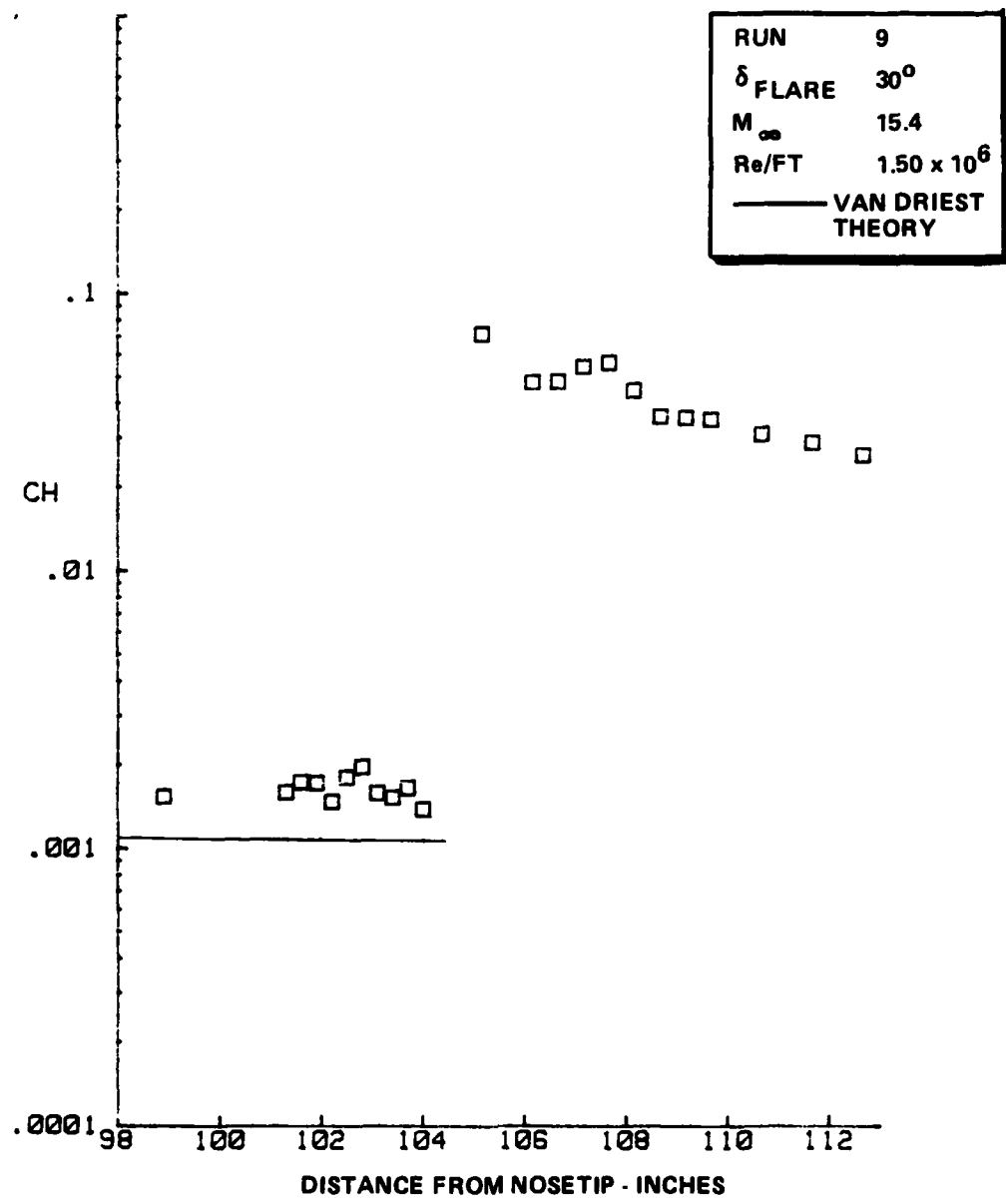


Figure 36b DISTRIBUTION OF HEAT TRANSFER IN ATTACHED FLOW OVER THE LARGE  $6^\circ$  CONE/ $30^\circ$  FLARE CONFIGURATION

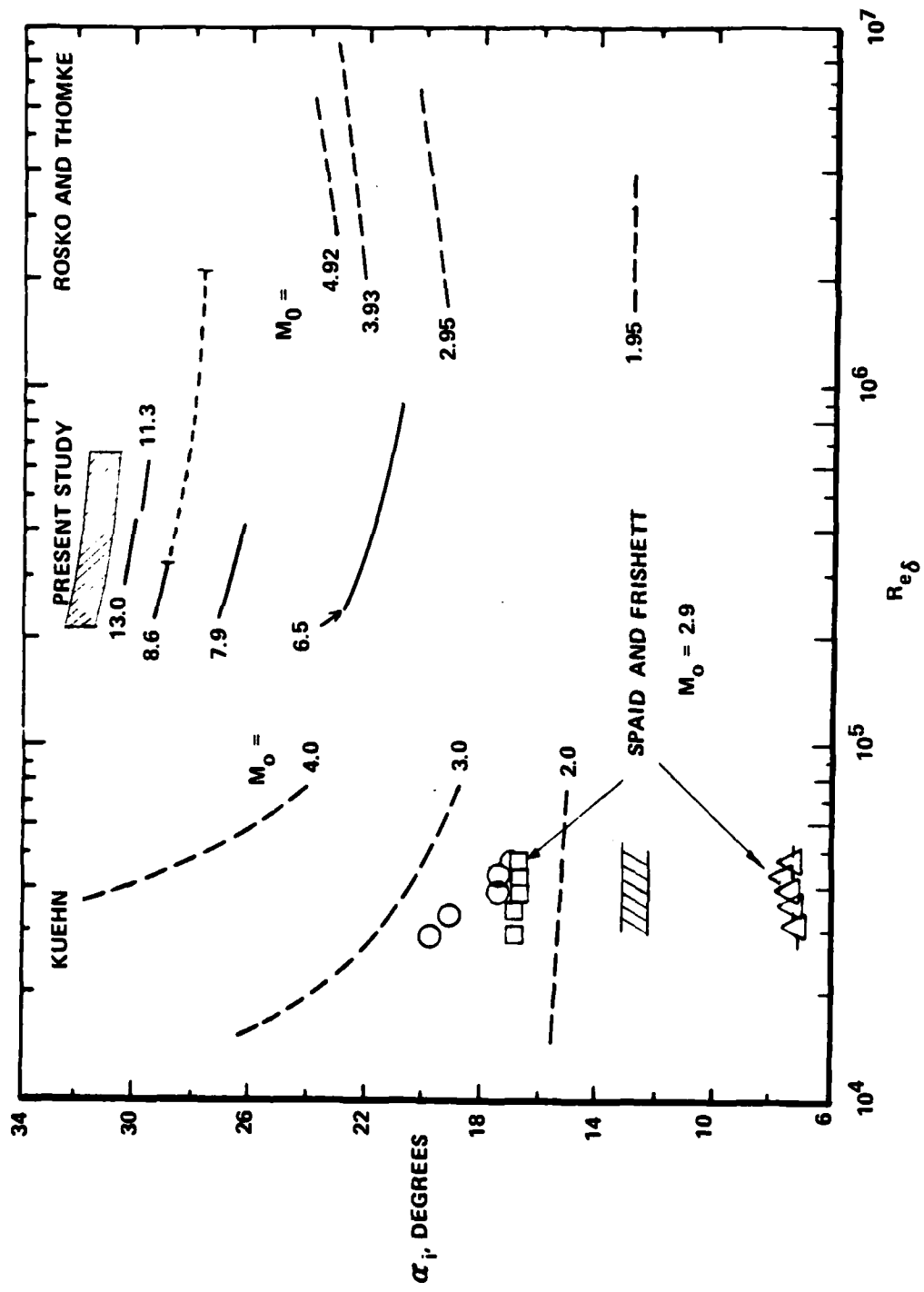


Figure 37 WEDGE ANGLE TO INDUCED INCIPIENT SEPARATION

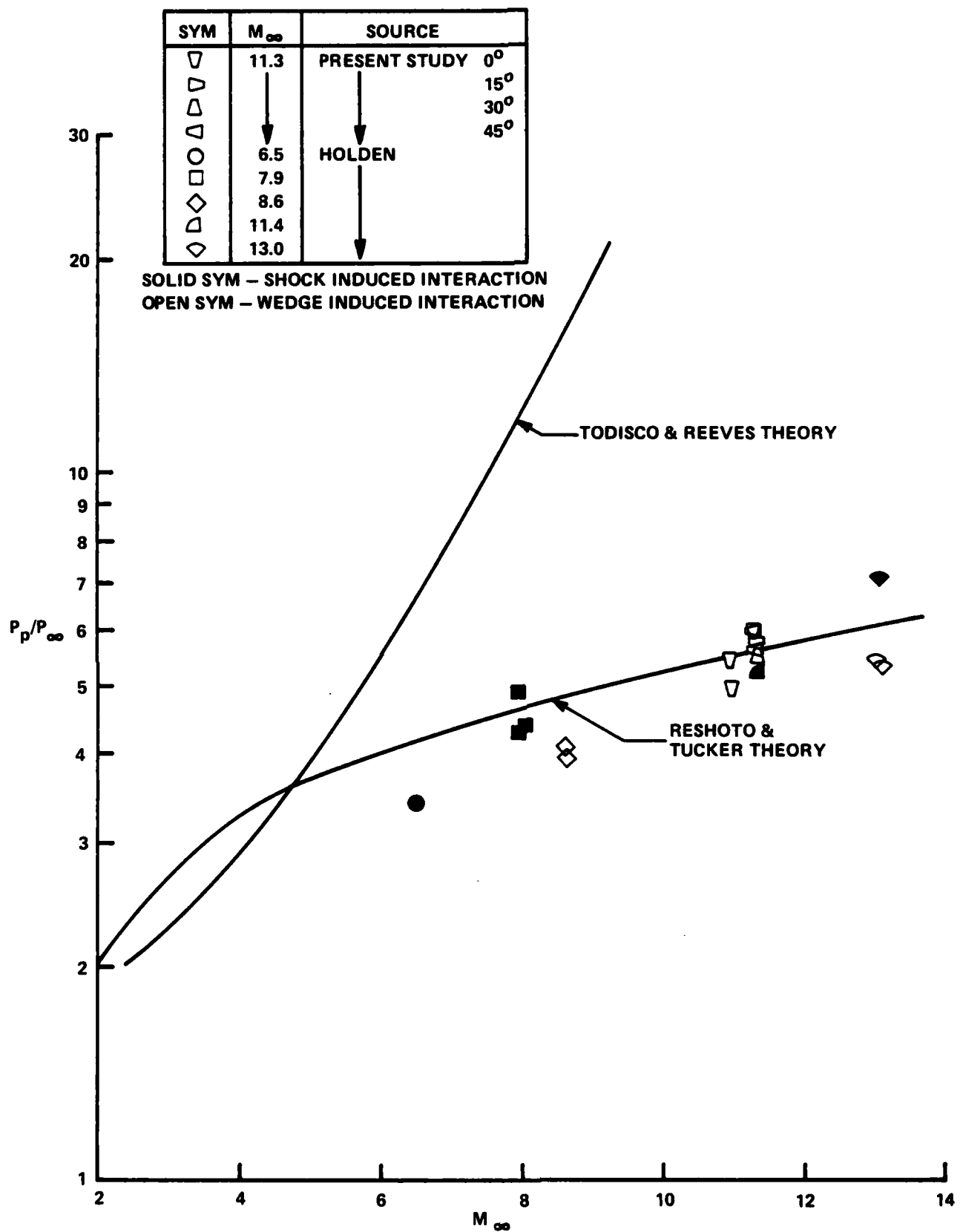


Figure 38 CORRELATION OF PLATEAU PRESSURE MEASUREMENTS ON 6° CONE/36° FLARE CONFIGURATION WITH EARLIER MEASUREMENTS

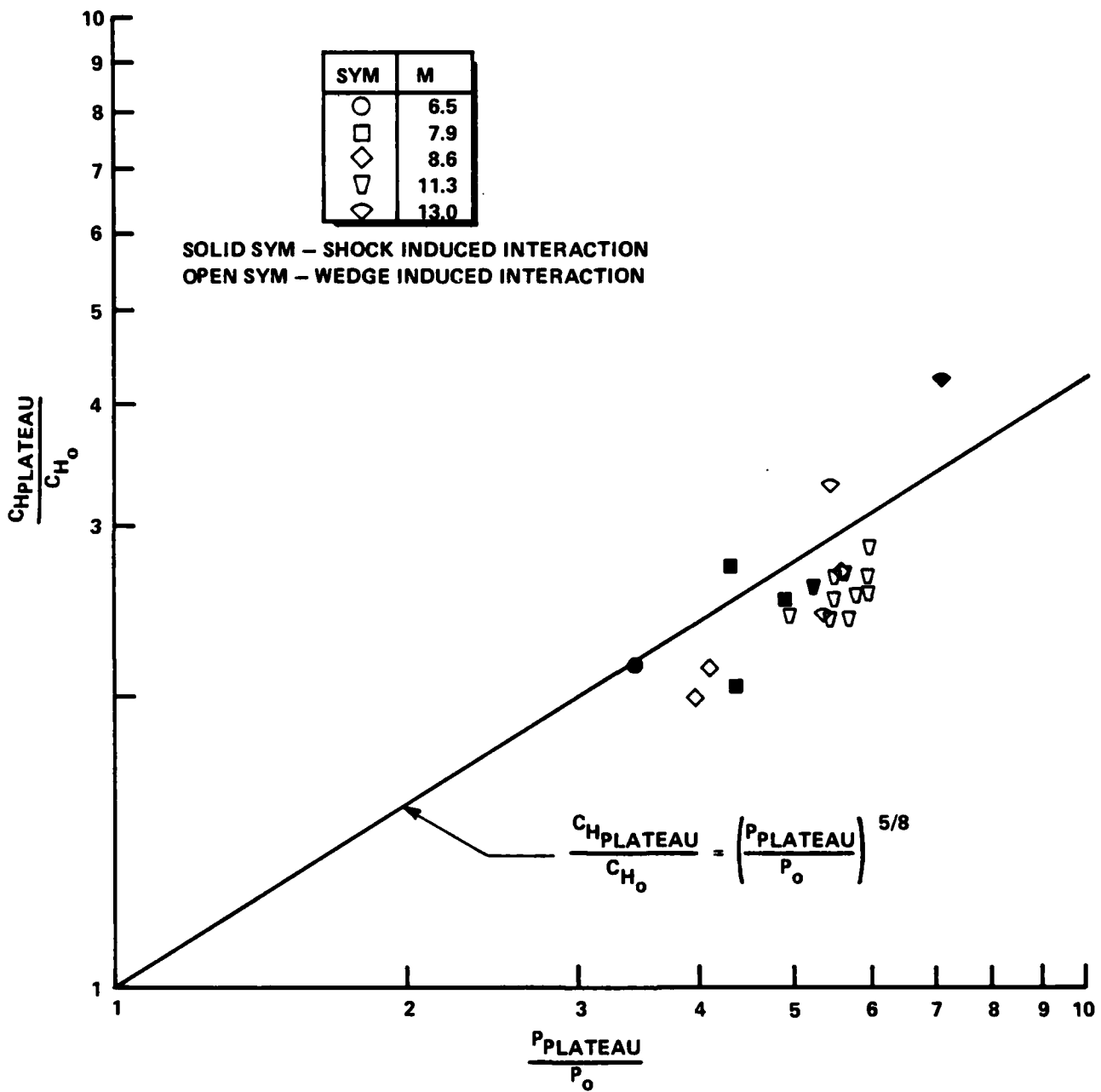


Figure 39 CORRELATION OF PLATEAU HEATING AND PRESSURE MEASUREMENT ON CONE/FLARE CONFIGURATION WITH EARLIER MEASUREMENTS

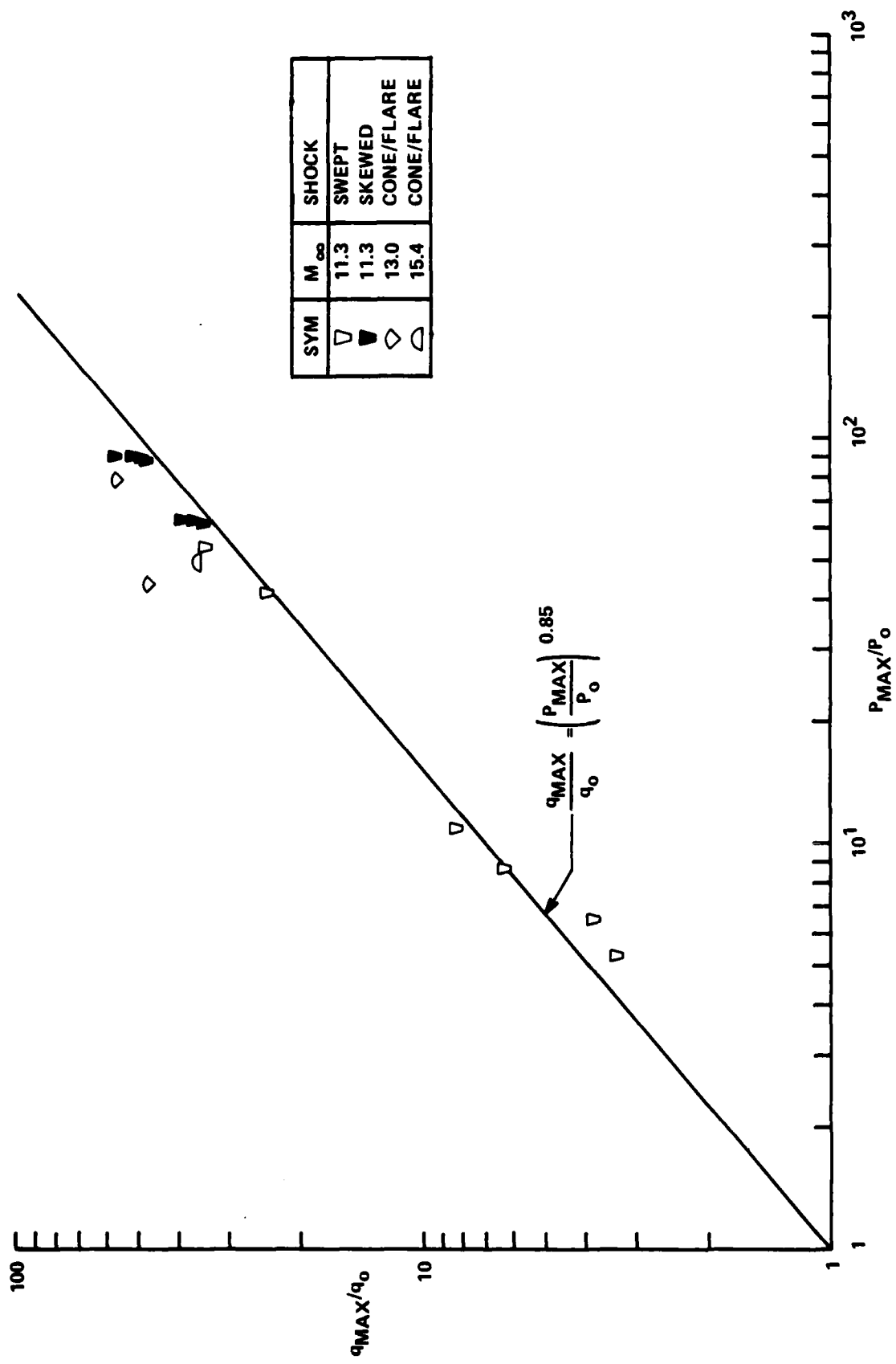


Figure 40 CORRELATION OF PEAK HEATING & PRESSURE MEASUREMENT ON CONE/FLARE CONFIGURATION WITH EARLIER MEASUREMENTS

### Conclusions

Experimental studies have been conducted to examine the characteristics of two- and three-dimensional flows induced by (i) skewed-oblique-shock/turbulent boundary layer interaction, and (ii) the three-dimensional viscous/inviscid interaction in the corner formed between a flat plate and a vertical fin, and (iii) the viscous/inviscid interaction at a cone/flare junction. Both studies were conducted at Mach 11 for Reynolds numbers of up to  $50 \times 10^6$ , under highly-cooled wall conditions. Detailed distributions of heat transfer and pressure as well as schlieren photographs were obtained for a range of model configurations to examine both attached and separated flows. The principal objective of the skewed interaction studies was to determine the effects of crossflow on the size and properties of separated interaction regions. Keeping the strength of the interaction constant, we varied the degree of crossflow by skewing the oblique shock between 0 and 45 degrees to the flat plate's leading edge. These studies demonstrated that crossflow has little effect on the scale and properties of the separated interaction regions, which contrasts with the findings of Settles, et al., who in an analogous study at Mach 3 on adiabatic surfaces, found a sizeable increase in the scale of the interaction with increased crossflow. We also found the plateau pressure and the heat transfer in the plateau and reattachment regions to be unaffected by crossflow. Our measurements in corner flows demonstrated that a significantly larger shock generator angle is required to separate the turbulent boundary layer in a swept-shock interaction than would be predicted from the correlations of McCabe or Korkegi, based on measurements in supersonic flows over adiabatic walls. While the shock generator angle to induce incipient separation was significantly larger than would be predicted from earlier studies, the salient features of the separated interaction regions, the plateau pressure, the location and magnitude of the peak pressure and heating were in good agreement with simple scaling laws developed from the full data base. We did, however, observe that the plateau pressure did not vary significantly with the normal component of Mach number  $M_\infty \sin \theta$ .

In the preliminary studies of the shock wave/turbulent boundary layer interaction at a cone/flare junction we obtained detailed measurements of the distribution of heat transfer and pressure through both attached and separated interaction regions at Reynolds numbers up to  $80 \times 10^6$  based on the length ahead of the interaction. The general characteristics of these interaction regions, the pressure rise to induce incipient separation, and the pressure and heating in the plateau and reattachment regions were

in general agreement with the semi-empirical prediction methods based on our earlier measurements at lower Reynolds number in two- and three-dimensional flows. Most importantly these experiments have verified the use of the very large cone/flare model as well as provided information on gross size and structure of the interaction regions which is invaluable in the design of subsequent studies to examine the structure of this flowfield in detail.

### References

1. Howarth, L., "The Propagation of Steady Disturbances in a Supersonic Stream Bounded on One Side by a Parallel Subsonic Stream," Proc. Camb. Phi. Soc. 1947, 44, Part 3.
2. Oswatitsch, K. and Wieghardt, K., "Theoretical Analysis of Stationary Potential Flows and Boundary-Layers at High Speed," German Wartime Report, 1941. Translated as N.A.C.A. TM. 1189.
3. Lighthill, M.J., "On Boundary-Layers and Upstream Influence. Part II. Supersonic Flows Without Separation," P.R.S.A., 1953, 217, 478.
4. Crocco, L. and Lees, L., "A Mixing Theory for the Interaction between Dissipative Flows and Nearly Isentropic Streams," J. Aero. Sci., Vol. 19, No. 10, pp. 649-676, October 1972.
5. Glick, H.S., "Modified Crocco-Lees Mixing Theory for Supersonic Separated and Reattaching Flows," J. Aero. Sci., Vol. 29, No. 10, pp. 1238-1244, October 1962.
6. Bray, K.N.C, Gadd, G.E. and Woodger, M., "Some Calculations by the Crocco-Lees and Other Methods of Interactions Between Shock Waves and Laminar Boundary Layer, Including Effects of Heat Transfer and Suction," A.R.C. Report No. C.P. 556 (1960).
7. Honda, M., "A Theoretical Investigation of the Interaction Between Shock Waves and Boundary Layers," J. Aero/Space Sci. 25, pp. 667-678, November 1958, Japan Tokyo Univ. Rep. Inst. High Speed Mech. 8, 1957, pp. 109-130.
8. Lees, L. and Reeves, B.L., "Supersonic Separated and Reattaching Laminar Flows: I. General Theory and Application to Adiabatic Boundary Layer-Shock Wave Interactions," GALCIT Tech. Report No. 3 (October 1963).

9. Holden, M.S., "An Analytical Study of Separated Flow Induced Shock Wave-Boundary Layer Interaction," Calspan Report No. AI-1972-A-3 (December 1965).
10. Holden, M.S. and Moselle, J.R., "Theoretical and Experimental Studies of the Shock Wave-Boundary Layer Interaction on Compression Surfaces in Hypersonic Flow," Calspan Report AF-2410-A-1 (October 1969); also ARL 70-0002 (January 1970).
11. Stalker, R.J., "The Pressure Rise at Shock-Induced Turbulent Boundary Layer Separation in Three-Dimensional Supersonic Flow," J. Aeronautical Science, Vol. 24, No. 7, pp. 547, July 1957.
12. Stanbrook, A., "An Experimental Study of the Glancing Interaction Between a Shock Wave and a Turbulent Boundary Layer," ARC CP 555, 1961.
13. McCabe, A., "The Three-Dimensional Interaction of a Shock Wave with a Turbulent Boundary Layer," Aeronautical Quarterly, Vol. XVII, pp. 231-252, August 1966.
14. Peake, D.J. and Rainbird, W.J., "The Three-Dimensional Separation of a Turbulent Boundary Layer by a Skewed Shock Wave and Its Control by the Use of Tangential Air Injection," AGARD CP-168, May 1975.
15. Oskam, B., Vas, I.E., and Bogdonoff, S.M., "Oblique Shock Wave/Turbulent Boundary Layer Interactions in Three-Dimensions at Mach 3, Part I," AFFDL-TR-76-48, June 1976.
16. Cousteix, J.A. and Houdeville, R., "Epaissement et Separation d'une Couche Limite Turbulente Soumise en Interaction avec un Choc Oblique," La Recherche Aerospatiale, No. 1, pp. 1-11, Jan./Feb. 1976.
17. Dolling, D.S. and Bogdonoff, S.M., "An Experimental Investigation of the Unsteady Behavior of Blunt Fin-Induced Shock Wave Turbulent Boundary Layer Interactions," AIAA-81-1287, 14th Fluid and Plasma Dynamics Conference, June 23-25, 1981.

18. Dolling, D.S. and Bogdonoff, S.M., "Upstream Influence Scaling of Sharp Fin-Induced Shock Wave Turbulent Boundary Layer Interactions," AIAA Paper 81-0336, AIAA 19th Aerospace Sciences Meeting, January 1981.
19. Dolling D.S. and Murphy, M., "Wall Pressure Fluctuations in a Supersonic Separated Compression Ramp Flowfield," AIAA-82-0986, AIAA/ASME 3rd Joint Thermophysics, Fluids, Plasma and Heat Transfer Conference, June 7-11, 1982.
20. Dolling, D.S., "Effects of Mach Number in Sharp Fin-Induced Shock Wave Turbulent Boundary Layer Interaction," AIAA-84-0095, 22nd Aerospace Sciences Meeting, Jan. 9-12, 1984.
21. Korkegi, R.H., "A Simple Correlation for Incipient Turbulent Boundary-Layer Separation Due to a Skewed Shock Wave," AIAA Journal, Vol. 11, No. 11, pp. 1578-1579, Nov. 1973.
22. Goldberg, T.J., "Three-dimensional Separation for Interaction of Shock Waves with Turbulent Boundary Layers," AIAA Journal, Vol. 11, No. 11, pp. 1573-1575, November 1973.
23. Newmann, R.D. and Burke, G., "The Influence of Shock Wave-Boundary Layer Effects on the Design of Hypersonic Aircraft," AFFDL-TR-68-152, USAF Flight Dynamics Laboratory, 1968.
24. Token, K.H., "Heat Transfer Due to Shock Wave Turbulent Boundary Layer Interactions on High Speed Weapon Systems," AFFDL-TR-74-77, April 1974.
25. Scuderi, L.F., "Expressions for Predicting 3D Shock Wave-Turbulent Boundary Layer Interaction Pressures and Heating Rates," AIAA Paper 78-162, January 1978.
26. Hung, C.M. and MacCormack, R.W., "Numerical Solution of Three-Dimensional Shock Wave and Turbulent Boundary Layer Interaction," AIAA Paper 78-161, January 1978.

27. Horstmann, C.C. and Hung, C.M., "Computations of Three-Dimensional Turbulent Separated Flows at Supersonic Speeds," AIAA Paper 79-2, January 1979.
28. Shang, J.S., Hankey, W.L., and Petty, J.S., "Three-Dimensional Supersonic Interacting Turbulent Flow Along a Corner," AIAA Paper 78-1210, July 1978; also AIAA Journal, Vol. 17, No. 7, pp. 706-713, July 1979.
29. Settles, G.S. and Horstmann, C.C., "Flowfield Scaling of a Swept Compression Corner Interaction—A Comparison of Experiment and Computation," AIAA-84-0096, 22nd Aerospace Sciences Meeting, January 9-12, 1984.
30. Ericsson, L.E., Reding, J.P., and Guenther, R.A., "Effects of Shock-Induced Separation," Lockheed Missiles and Space Co., Sunnyvale, CA, L-87-69-1, July 1969.
31. Settles, G.S., and Perkins, J.J., "Upstream Influence Scaling of 2D & 3D Shock/Turbulent Boundary Layer Interactions at Compression Corners," AIAA-81-0334, 19th Aerospace Sciences Meeting, January 12-15, 1981.
32. Settles, G.S. and Teng, H.Y., "Flow Visualization of Separated 3D Shock Wave/Turbulent Boundary Layer Interactions," AIAA-82-0229, 20th Aerospace Sciences Meeting, January 11-14, 1982.
33. Reshotko, E., and Tucker, M., "Effect of a Discontinuity on Turbulent Boundary Layer Thickness Parameters With Application to Shock Induced Separation," NACA, TN3454, 1955.
34. Green, J.E. "Interactions Between Shock Waves and Turbulent Boundary Layers Progress in Aeronautical Sciences," Vol. II, Pergamon Press at Oxford, pp 235-340, 1970.